UNIVERSITA' DEGLI STUDI DI MILANO

PhD Program in

Integrative Biomedical Research

XXX Cycle

In-vivo and *in-vitro* electrophysiological characterization of the cardiac pacemaker activity during aging and in the presence of the Traditional Chinese Medicine drug TMYX

Tutor: Prof. Mirko Baruscotti

Coordinator: Prof.ssa Chiarella Sforza

Dott.ssa Chiara Piantoni

Matr: R10852

Anno Accademico 2016-2017

Ai miei Maestri di Vita,

Ai miei Maestri di Scienza.

INDEX

INDEX **3**
PREFACE **5**
1) HCN CHANNELS EXPRESSION IN HUMAN LEUKOCYTES. 5
2) AGE-DEPENDENT CHANGES IN MURINE CARDIAC PACEMAKER ACTIVITY 5
3) MODE OF ACTION OF THE TRADITIONAL CHINESE MEDICINE DRUG TMYX ON PACEMAKER ACTIVITY IN FREELY-MOVING MICE AND IN ISOLATED SAN CELLS 6
4) ELECTROPHYSIOLOGICAL CHARACTERIZATION OF A COMPOUND HETEROZYGOSITY MUTATION OF THE CARDIAC SODIUM CHANNEL NAV1.5 8
GENERAL INTRODUCTION **9**
ELECTRICAL ACTIVITY OF THE HEART 9
The conduction system of the heart 9
Figure 1. The conduction system of the heart. 9
Action potential 10
Figure 2. Pacemaker and ventricular action potential. 10
The funny current 11
Figure 3. Effects of the autonomic modulators on action potentials and I_f current. 12
HCN channels 12
Figure 4. HCN channels structure. 13
The electrocardiogram 13
Fig.5. Representation of a normal electrocardiogram. 13
Autonomic control of heart rate 14
Figure 6. Autonomic innervation of the heart. 14
Heart rate variability 15

AGE-DEPENDENT CHANGES IN MURINE CARDIAC PACEMAKER ACTIVITY **16**

INTRODUCTION **16**
AIMS **18**
RESULTS **19**
Figure 1. Basal HR does not change between young and old mice. 19
Figure 2. The injection of a saline solution does not change HR. 20
Figure 3. Intrinsic heart rate decreases with aging. 21
Figure 4. Funny current density decreases with aging. 21
Figure 5. Aging causes a leftward shift of the I_f activation curve. 22
Figure 6. The sympatho-vagal system is balanced in the young and unbalanced in the old mice. 23
Figure 7. Heart rate variability decreases with aging. 24
Figure 8. Maximal heart rate decreases with aging while adrenergic response does not. 25
Figure 9. The maximal muscarinic response seems to be similar between young and old animals, while the recovery seems different. 26
DISCUSSION **27**

MODE OF ACTION OF THE TRADITIONAL CHINESE MEDICINE DRUG TMYX ON PACEMAKER ACTIVITY IN FREELY-MOVING MICE AND IN ISOLATED SAN CELLS **31**

INTRODUCTION **31**
STATE OF ART 31
Figure 1. TMYX reduces AP rate of rabbit single SAN cells. 32

Figure 2. TMYX reduces the I_f current availability..... 33
AIMS..... 34
RESULTS..... 35
In-vitro experiments:..... 35
Figure 1. TMYX and ACh share a common mechanism..... 35
Figure 2. TMYX does not activate muscarinic receptors..... 37
Figure 3. The enhancement of cAMP pathway reduces the TMYX action on the I_f current..... 38
Figure 4. TMYX does not affect the probability of HCN channels opening..... 39
Figure 5. TMYX does not reduce the I_f current in inside-out configuration..... 40
Figure 6. TMYX reduces the I_f current in inside-out configuration when delivered in the presence of cAMP 1 μM..... 41
Figure 7. TMYX reduces the I_f current in inside-out configuration when delivered in the presence of cAMP 10 μM..... 42
Figure 8. TMYX does not reduce the I_f current in inside-out configuration when delivered in the presence of saturated concentration of cAMP..... 43
In-vivo experiments:..... 43
Figure 9. TMYX reduces the intrinsic heart rate in freely-moving mice..... 44
Figure 10. TMYX accelerates heart rate in freely-moving mice..... 45
Figure 11. TMYX accelerates heart rate in the presence of the only sympathetic system while it decreases heart rate in the presence of parasympathetic system..... 46
Figure 12. Guanethidine antagonizes the tachycardic action of TMYX..... 47
DISCUSSION..... 48
GENERAL CONCLUSIONS..... 52
MATERIALS AND METHODS..... 53
ANIMALS..... 53
IN-VIVO EXPERIMENTS..... 53
Radio-telemetry system..... 53
Radio-transmitter implantation..... 53
Experimental protocols..... 53
Data analysis:..... 54
IN-VITRO EXPERIMENTS..... 54
Single sinoatrial node cells isolation..... 54
Electrophysiological setup..... 55
Patch-clamp solutions..... 55
Data analysis and protocols..... 55
Action Potential..... 56
Funny current..... 56
Funny current activation curve..... 56
Current density..... 56
Inside-out configuration..... 57
BIBLIOGRAPHY..... 58

PREFACE

During my Ph.D. course, I have been involved in four different projects with different issues and aims, but with the common background of ion channels. In this introductory part I will briefly summarize the main points of each of them and in the following part of the thesis I will discuss more in detail the two that have achieved more completeness in these years.

1) HCN channels expression in human leukocytes.

Ivabradine is a heart rate-reducing agent, which specifically and selectively blocks pacemaker HCN channels. Strong evidence in the literature shows that Ivabradine also reduces inflammatory processes and the suggested mechanism of action is the modification of the vascular shear stress caused by the primary bradycardic effect of the drug[1,2].

Leukocytes, the key players of the immune response, express several ion channels ($K_{v1.3}$, $K_{Ca3.1}$, CRAC, TRPM4, ORAI1 and others) that control the functional state of the cell and are therefore involved in cell activation and inflammatory processes[3,4]. Since HCN channels are important determinants of the membrane potential in several excitable and non-excitable cell types[5], we investigated the presence of these channels in leukocytes.

Initial PCR experiments carried out in total human leukocytes led to the identification of all four HCN isoforms, although the signals were faint, and quantitative PCR revealed a stronger presence of HCN2 and HCN3 mRNA. Western Blot confirmed the presence of HCN2 and HCN4 protein signals in total leukocytes and of HCN3 in lymphocytes, and flow cytometry analysis revealed that granulocytes and lymphocytes were the major sources of the HCN3 signal.

Based on the identification of mRNA and protein I finally tested the effect of Ivabradine (1 μM) on the activation process of human total leukocytes. The results show a 29±9% (n=5) reduction in the activation readout parameters in the presence of Ivabradine. These results therefore raise the possibility that the mechanism by which Ivabradine reduces inflammation is a direct binding to HCN channels in human leukocytes and we therefore suggest that HCN channels may play a functional role in specific human leukocytes subpopulations. Future electrophysiological experiments will further investigate this possibility.

2) Age-dependent changes in murine cardiac pacemaker activity

Cardiovascular diseases (CDVs) are the main causes of death. The incidence of morbidity and mortality associated with CDVs increases exponentially in the elderly population due to the increase of both the number of old people and of the average lifespan (for example it is estimated that in the United States there will be 70 million people over the age of 65 by the year 2030,

representing almost 25% of the population,[6]. Amongst the age-dependent cardiovascular diseases, the sinoatrial node dysfunction has a primary role[7]; for this reason, there is a high interest in the study of the pathophysiological mechanisms that are at the basis of cardiac aging.

It is known that in humans during ageing there is a decline in maximum heart rate (MHR) and a reduction in the intrinsic heart rate (IHR)[8,9]; however basal heart rate (BHR) remains the same between the adults and the elderly[10]. We thus decided to better understand the age-associated mechanisms responsible for the changes in intrinsic and maximum heart rate but not in the basal heart rate, and we chose the mouse as a study model.

We therefore first confirmed that in our murine model the IHR, but not the basal HR, decreases with ageing; and we also noticed that in adult mice the IHR and the BHR were similar. We focused our studies on the *funny* current since it is a main contributor to pacemaking generation and modulation and we observed a reduction of the current density and a negative shift of the activation curve in the old animals. We then evaluated the influence of the autonomic system and we found that in adult mice both branches of the autonomic system contribute similarly to HR, though in opposite directions; old mice instead had a lower vagal tone, leading to a reduction in the overall HRV as assessed by spectral analysis, and an increased sympathetic tone, leading to a larger vulnerability to spontaneous arrhythmias compared to adult.

Our data highlight that this model recapitulates well the HR features observed in aged humans and can help understanding the mechanisms of the ageing-associated changes in heart chronotropism. The shift of the sympatho-vagal balance toward a sympathetic prevalence in the old animals may explain why, despite the difference in the intrinsic heart rate, the basal heart rate is similar between the two groups. While the current view is that the sympathetic increase is necessary to ensure the homeostatic balance of heart rate during ageing, it is also possible that the age-dependent increase of the sympathetic tone is the cause of the reduction of the intrinsic heart rate which therefore ultimately represents the compensatory effect.

3) Mode of action of the Traditional Chinese Medicine drug TMYX on pacemaker activity in freely-moving mice and in isolated SAN cells

The identification of novel pharmacological agents able to selectively reduce sinus rate has a strong interest in the clinic because of their potential use in the treatment of ischemic heart disease such as *angina pectoris*. Despite longstanding and intense investigation, at present there is only one such agent (Ivabradine) that has reached therapeutic application, since all other compounds tested had additional undesired side-effects[11,12].

Our laboratory has started few years ago a collaboration with the University of Tianjin (China) to

investigate the efficacy of the cardioactive compound Tongmai Yangxin (TMYX) which is currently used in the Traditional Chinese Medicine as a cardiac regulator[13].

Electrophysiological experiments performed on rabbit SA node cells have shown a dose-dependent slowing effect of TMYX on pacemaking action potential rate. The investigation of the effects of TMYX on the I_f current, the major contributor of diastolic depolarization phase, has revealed that at physiological potential the drug exerts a bradycardic action, thus confirming the effect on the spontaneous automaticity observed in SA node cells.

During my experimental work, I continued the characterization of the mechanism of action of this Traditional Chinese Medicine drug, working on two parallel aspects: 1) the evaluation of the systemic effect of TMYX and 2) the identification of the molecular mechanisms of the drug.

1) The systemic effect of TMYX was evaluated in freely-moving mice implanted with ECG transmitters. When TMYX was delivered during pharmacological blockade of either sympathetic alone or in combination with parasympathetic block, a deep bradycardia was observed, confirming the *in-vitro* bradycardic effect. However, quite surprisingly, when the drug was delivered (i.p. injection) during basal heart rate condition, the experiments show an increment of heart rate.

2) Our previous *in-vitro* experiments had revealed that TMYX acts directly on pacemaker SAN cells and blocks the pacemaker current. We therefore started a series of experiments aiming at the identification of the site of action of TMYX. Our experiments suggest that TMYX shares the modulatory pathway of ACh, but they also exclude that TMYX can bind to the M2 receptor because atropine does not alter the action of TMYX. We then performed inside-out experiments and demonstrated that TMYX does not have any action on the channel when cAMP is either completely absent or it is present at saturating high levels, while TMYX decreases the pacemaker current when cAMP is present at non-saturating levels. Taken together our results demonstrate the presence of at least two molecules that exert different actions: one is a bradycardic agent, whose effect is observed in isolated SAN cells and in the *in-vivo* model, and the other one is a systemic tachycardic agent, whose effect is observed in the absence of autonomic block. The bradycardic agent appears to behave as an antagonist of the sympathetic stimulation of heart rate. The antagonist action on the sympathetic activity is a key pharmacologic mechanism used by the so-called β-blocker drugs. These drugs are largely used to treat a large number of cardiac diseases including Coronary Artery Disease (CAD) and Heart Failure (HF). However, the often-undesired side effect of β-blockers is a decreased strength of contraction (inotropism) of the heart. According to our data it appears that the active molecule in the TMYX acts directly on the pacemaker channel by antagonizing the stimulating action of cAMP, while β-blockers slow heart rate by decreasing the cAMP levels. This direct antagonistic effect, rather than a block of cAMP production should decrease the heart rate

leaving unaltered the strength of contraction. We thus intend to identify and isolate the specific tachycardic/bradycardic molecules since they could have a strong impact in the clinical use.

4) Electrophysiological characterization of a compound heterozygosity mutation of the cardiac sodium channel Nav1.5

Mutations in SCN5A/Nav1.5 channel are associated with multiple cardiac diseases including long-QT syndrome type 3 (LQT3), Brugada Syndrome, Sinus Node Dysfunction (SND), etc[14,15]. Although considered separate entities, all these syndromes can be collectively called Na^+ channelopathies and, indeed quite often, they display mixed phenotypes.

We studied the case of a 2-years-old baby[16] with compound heterozygosity for paternal (Lys1578Asn) and maternal (Gly-1866fs) allele mutations of the α-subunit of SCN5A and presenting SND, atrial flutter recurrences, and drug induced long-QT syndrome, by assessing SCN5A wild type and mutated channels activity through electrophysiological analysis.

We first separately evaluated the effect of each mutation in a heterologous cell system (HEK293 cells). Our results show that both mutations cause a reduction in the sodium current compared to the wild type system and this evidence may justify the clinically observed bradycardia since this type of genotype (loss-of-function mutation of Na channels) - phenotype (bradycardia) link has already been observed. We will characterize the effect of the compound mutation with further experiments to better understand the clinical case of our patient.

GENERAL INTRODUCTION

As mentioned in the previous chapter, my thesis will particularly focus on the following two specific projects: "*Age-dependent changes in murine cardiac pacemaker activity*" and "*Mode of action of the Traditional Chinese Medicine drug TMYX on pacemaker activity in freely-moving mice and in isolated SAN cells*" and therefore a general introduction is presented here.

The study of the electrophysiological properties of the cardiac pacemaker activity during aging or in the presence of the Traditional Chinese Medicine drug TMYX represents well the concept of integrated biomedical research. These two studies have indeed the common general aim to unravel the molecular and systemic mechanisms at the basis of cardiac rhythm. In both studies the main actors involved are the sinoatrial node, the natural pacemaker of the heart, and the autonomic nervous system, one of the major regulator of cardiac rhythm. As part of an integrated research I studied the patho-physiological aspects of cardiac pacing during aging, and the mechanisms of action of a compound of the Traditional Chinese Medicine which is able to control heart rate in diseased states.

Electrical activity of the heart

The heart is a muscle that works like a pump; its function is to pump blood through the body via the circulatory system. Cardiac tissue is mainly composed by two types of tissue: myocytes mainly involved in contractile activity, known as *working myocardium*, and myocytes dedicated to electrical impulse generation and conduction, known as *conduction system.*

The conduction system of the heart

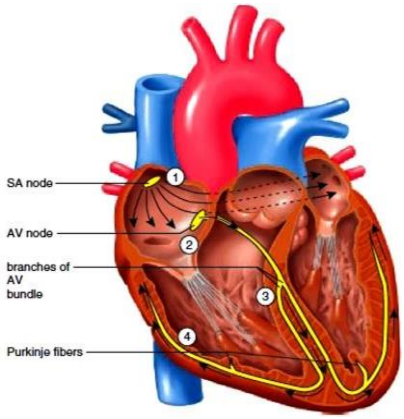

Figure 1. The conduction system of the heart. 1) The SAN generates impulse; 2) the impulse travels through the AVN and it slows down; 3) excitation spreads down the bundle of His; 4) Purkinje fibers distribute excitation through ventricular myocardium.

The cardiac conduction system is a specialized structure with the function of generating and leading impulses throughout the heart. This system is made up of specialized cells able to spontaneously generate and transfer the electric impulse to the working myocardium of the various chambers of the heart.

The cardiac conduction system is composed by different tissues:

1. The sinoatrial node (SAN);
2. The atrioventricular node (AVN);
3. The bundle of His;
4. The Purkinje fibers.

The SAN consists of a group of cells located in the wall of the right atrium of the heart. It is the tissue where the electrical impulse is generated; for this reason is also known as the natural pacemaker of the heart. The electrical signal is spread to adjacent atrial myocardial cells through the gap junctions, while it travels from the atria to the ventricle through a group of specialized cells of the conduction system, called atrioventricular node (AVN). Here the impulse is decelerated and then reaches the bundle of His, that is divided into right and left branches, which continue with the Purkinje fibers within the ventricular walls. These fibers allow the synchronized contraction of the ventricles.

The impulse generated by the sinoatrial node and transmitted through the heart is called *action potential*.

Action potential

The action potential represents the changes in the voltage created by a sequence of ion fluxes through specialized channels in the membrane of single cardiomyocytes.

Different regions of the heart have different action potentials; all action potentials recorded are grouped into two main types: 1) “slow response”, observed in the SAN and in the AVN and 2) “fast response”, typical of atrial and ventricular myocardium.

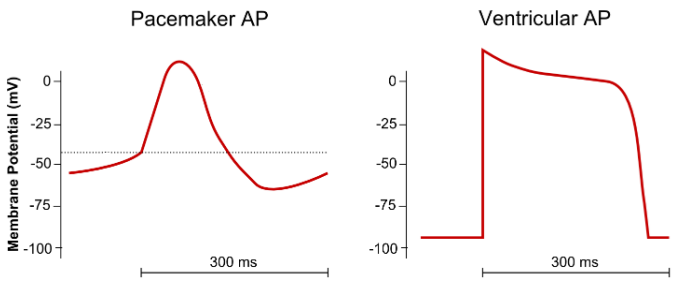

Figure 2. Pacemaker and ventricular action potential. The pacemaker cells have a typical slow response action potential, while the ventricular cells show an action potential with the feature of the fast one.

During diastole the membrane potential of a ventricular cell is maintained at the resting value of about -90 mV by the presence of the inward rectifier current (I_{K1}) until a new depolarizing stimulus arrives. In the SAN instead there is no diastolic resting electrical state since the cell reaches its most negative value only for a small fraction of time and then immediately slowly depolarizes. The most negative potential reached in the SAN (maximum diastolic potential, MDP) is about -60 mV. This value is determined by the outward potassium currents (I_{Kr}, I_{Ks}) and by the activation of the inward I_f current (see the paragraph below). The slow diastolic depolarization which follows the attainment of the MDP is typical of nodal cells and gives them the characteristic of automaticity. The last of the diastolic depolarization is also sustained by transient or T-type Ca^{2+} ($Ca_V3.1$) channels, and by the long-lasting, or L-type Ca^{2+} ($Ca_V1.3$) channels[17]. In addition another L-type Ca^{2+} ($Ca_V1.2$) is also present and contributes to the upstroke phase of the action potential[18].

Differently, non-pacemaker cells are depolarized from -90 mV to a threshold voltage of about -70 mV thanks to an external stimulus and the following rapid depolarizing phase is sustained by an increase in the Na^+ current. After this depolarizing phase in the pacemaker cells there is only a hyperpolarization (also known as phase 3) since K^+ channels open and the L-type Ca^{2+} channels become inactivated.

Ventricular and atrial cardiomyocytes have instead 3 phases after the rapid depolarization: phase 1, with an initial repolarization caused by the opening of a transient outward K^+ channel (I_{Kto}); phase 2, the plateau phase, sustained by the balance of inward calcium current generated by L-type calcium channels and outward potassium currents (I_{Krs}, I_{Ks}), which allow the maintenance of the membrane potential near 0 mV for about 200 ms; phase 3, the repolarization to the resting value, due to the inactivation of L-type calcium channels and the active presence of rapid (I_{Kr}) and slow (I_{Ks}) repolarizing current.

The funny current

The function of sinoatrial node cells is to generate spontaneous action potentials. The automaticity typical of these cells is due to the diastolic depolarization, determined mostly by the activation of the *funny* (I_f) current[19]. This current has unusual ("*funny*") characteristics[20]: i) activation in hyperpolarization, at voltages of about -40/-45 mV; ii) mixed sodium and potassium conduction, with a resulting reversal potential of about -10/-20 mV[19,21] and iii) increase of the probability of channel opening by a direct binding of cyclic AMP (cAMP)[22], which is modulated by autonomic neurotransmitters activation.

Cyclic AMP is a second messenger that modulates several ion channels by a mechanism involving PKA-dependent phosphorylation. The peculiarity of the cAMP modulation of the I_f current is that

cAMP directly interacts with the channels. In sinoatrial node cells the increase/decrease of intracellular cAMP shifts the I_f activation curve to more positive/negative voltages. By activating β-adrenergic (β1 and β2) and muscarinic M2 receptors, respectively, the sympathetic and parasympathetic neurotransmitters control the cytosolic concentration of the second messenger cAMP. This induces an increase/decrease of the net inward current causing an increment/reduction of the steepness of the diastolic depolarization and a consequent increase/decrease of firing rate, respectively.

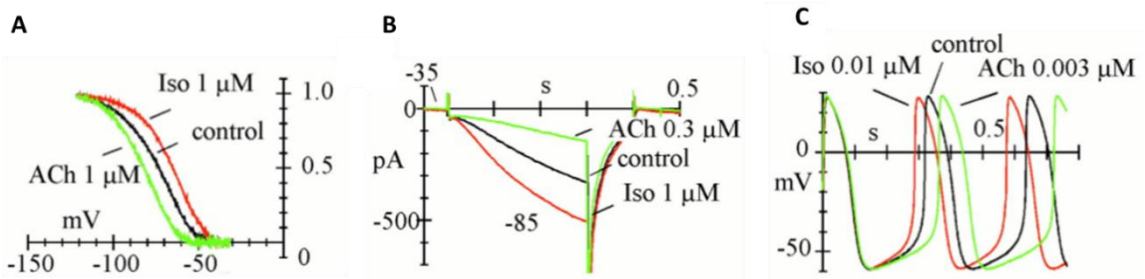

Figure 3. Effects of the autonomic modulators on action potentials and I_f current. (**A**) Acetylcholine (ACh) and Isoprenaline (Iso) induce a shift of the activation curve to more negative/positive voltages. (**B**) The I_f current amplitude increases with Iso and decreases with Ach. (**C**) The administration of the autonomic modulators induces acceleration (Iso) and deceleration (ACh) of spontaneous rate of action potentials.

HCN channels

The molecular correlate of the I_f current is represented by the hyperpolarization-activated cyclic nucleotide-gated (HCN) channels[23]. To date four homologous HCN channel subunits (HCN1-4) have been cloned. They are classified as members of the voltage-gated K^+ (Kv) and CNG channels: they have a tetrameric composition[23,24], and each subunit is composed of 6 transmembrane domains (S1–6). They have a positive charged S4 domain, with the function of voltage sensor[25,26] and an ion-conducting pore (S5–S6). In the C terminus the channels carry a cyclic nucleotide-binding domain (CNBD). The four HCN channel subtypes show different characteristics (time constants, steady-state, voltage dependence and cAMP modulation)[27]. HCN1 has the fastest kinetics with a strong voltage dependence (from 30 to 300 ms at -140 to -95 mV) and the most positive $V_{1/2}$ (- 70/-90 mV). It is less sensitive to cAMP (shift: +2/+7 mV) than HCN2 and HCN4.

HCN4 is the channel with the slowest opening kinetics (~3 s at -95 mV); HCN2 has intermediate values of time of activation (from 150 ms to 1 s). Both HCN2 and HCN4 are strongly sensitive to cAMP (shift: +10/+25 mV) . Few works have been done on HCN3; it shows kinetics between those of HCN2 and HCN4; its modulation by cAMP is very limited[23,27-34].

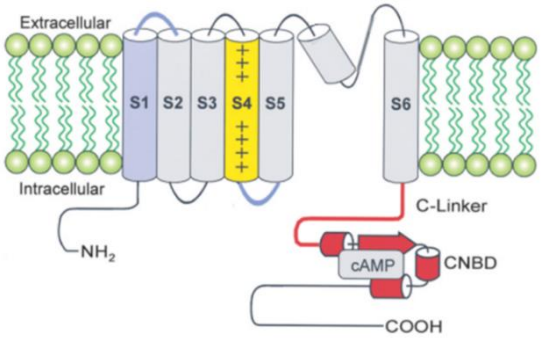

Figure 4. HCN channels structure. Each one of the four subunits is composed of 6 transmembrane domains (S1–6). S4 is the charged domain, with the function of voltage sensor. S5 and S6 domains form the conducting pore. In the C terminus the channels carry a cyclic nucleotide-binding domain (CNBD).

The electrocardiogram

The electrical activity of the heart can be recorded by electrodes placed on the skin. The trace obtained by this registration is called electrocardiogram (ECG).

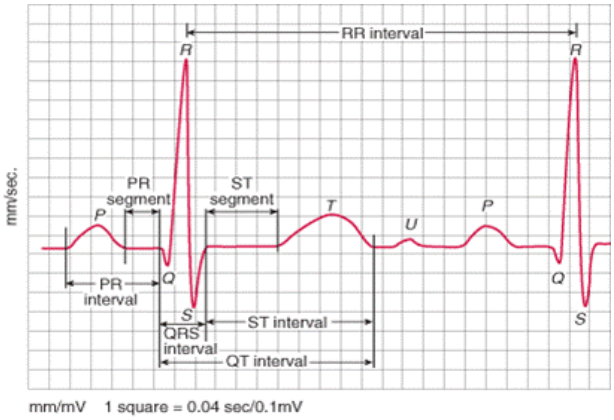

Fig.5. Representation of a normal electrocardiogram. A normal ECG is composed of P wave, QRS complex and T wave. The distance between two consecutive R peak is used as a measure of heart rate.

Normal ECG is composed of: P wave, that represents atrial depolarization from the SAN to the AVN and from the right atrium to the left atrium; QRS complex, which stands for the rapid depolarization of the right and left ventricles; T wave, that reflects ventricular repolarization. The term heart rate normally refers to the rate of ventricular contractions. Ventricular rate can be therefore determined by measuring the time intervals between the QRS complex, which is done by looking at the R-R intervals.

Autonomic control of heart rate

Heart rate is controlled by the two branches of the autonomic nervous system: the parasympathetic nervous system (PNS) and the sympathetic nervous system (SNS).

The parasympathetic system mainly innervates the sinoatrial and the atrioventricular nodes. Atrial and ventricular muscles are less influenced by PNS. The sympathetic system innervates the entire heart.

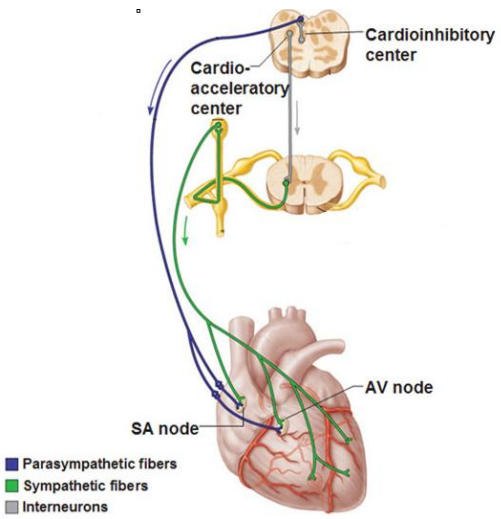

Figure 6. Autonomic innervation of the heart. The parasympathetic system mainly innervates the sinoatrial and the atrioventricular nodes, while the sympathetic system innervates the entire heart.

The parasympathetic nervous system (PNS) releases acetylcholine, with two main effects on the heart: 1) decrease of SAN rate and 2) reduction of AVN fibers excitability, slowing down impulse transmission. Acetylcholine induces a hyperpolarization of the membrane of the fibers due to a rapid diffusion of K^+ ions outwards. In the SAN the resting potential becomes more negative and more time is needed to reach the threshold of excitation. The hyperpolarization of the AVN induces a delay in the pulse conduction.

SNS releases catecholamines (epinephrine and norepinephrine) with opposite effects to those of PNS:

1) increase of SAN rate; 2) increase of impulse conduction and general excitability and 3) increase of atrial and ventricular force of contraction.

The mechanism is the opposite of that of the parasympathetic innervation, with a depolarization of the membrane due to an increased permeability to Na^+ and Ca^{2+}.

The neurotransmitters of the autonomic nervous system bind specific receptors on the cell membranes of the effector tissue. All adrenergic receptors (mediators of the Sympathetic Nervous System) and muscarinic receptors (mediators of the Parasympathetic Nervous System) are coupled to G proteins.

Noradrenaline is released from sympathetic presynaptic terminals and binds to β2-receptors. The binding causes an increase in the production of the intracellular cAMP concentration by adenylate cyclase, a process mediated by a stimulatory Gs protein. On the other hand, acetylcholine is released from parasympathetic presynaptic terminals and binds M2-muscarinic receptors inducing a decrease in the intracellular cAMP concentration[35]. cAMP acts as a second messenger increasing the activity of the Protein Kinase A (PKA) which, in turn, phosphorylate several proteins on the membrane, such as the L-type Ca^{2+} channels[36,37]. In addition, cAMP increases the opening chance of HCN channels by direct binding to them in a PKA-independent way[22]. Phosphodiesterases (PDE) lowers the cAMP concentration by converting it to 5-AMP , thus reducing several currents, such as the I_{CaL} and the I_f current.

Heart rate variability

Heart rate variability (HRV) is the analysis of beat-to-beat variation in heart rate (R-R intervals) under resting conditions. The variations are either quantified by simple statistical methods (time domain analysis) or by using computer algorithms to detect slow (low-frequency modulations) and fast (high-frequency modulations) changes occurring from beat to beat. These modulations reflect the balance between sympathetic (low-frequency modulations) and parasympathetic (high-frequency modulations) input to the heart.

HRV is influenced by several physiologic and diseased conditions. Decreased variability suggests decreased vagal input and increased sympathetic input, which predict increased risk of arrhythmias and mortality[38].

Age-dependent changes in murine cardiac pacemaker activity

INTRODUCTION

Aging represents one of the major risk factors for cardiovascular diseases.

The incidence of morbidity and mortality associated with cardiovascular diseases increases exponentially in the elderly population and it has been predicted that by 2035 almost 25% of the population will be over 65 years old[6].

Sinus Node Disease is one of the predominant age-related cardiovascular diseases and the Sick Sinus Syndrome affects 1 in 600 patients with a mean age between 73 and 76 years old[7].

The causes of SND in the elderly population are various and often complex; furthermore, in many cases the identification of the mechanisms at the basis of these pathologies are still lacking. For this reason, there is a high interest in the study of the pathophysiological mechanisms that are at the basis of cardiac aging.

One of the main finding about cardiac aging is the observation that the intrinsic heart rate decreases with aging. Several studies have been carried out, both on humans and on mice, to investigate this aspect[8,9,39]. Intrinsic heart rate is the heart rate in the absence of the influences of the autonomic nervous system and therefore the reduction of the intrinsic heart rate reflects an impairment of the sinoatrial node function per se.

To verify this aspect, patch-clamp experiments were carried out on single pacemaker cells with the aim of evaluating the activity of SAN cells during aging in the absence of potential influences operated by surrounding tissue (for example the "sink" activity of the right atrium). These experiments demonstrated that nodal cell AP firing rate is reduced with aging and this finding explains the reduction of heart rate measured in the presence of autonomic block[39]. A careful analysis of these data revealed that the slowing of AP rate is due to a decrease of the steepness of the early diastolic depolarization. As explained in the general introduction of this thesis, this phase of the action potential is sustained by the funny current, also known as pacemaker current. Larson et al.[39] demonstrated that the decrease in the slope of the diastolic depolarization results from a reduced current density and a hyperpolarizing shift of the activation curve of the I_f current.

Another important aspect of cardiac aging is the reduction of the maximum heart rate attainable during maximal adrenergic stimulation; the proposed explanation for this event is associated both to the reduction of the intrinsic heart rate and to the reduction of the responsiveness to β-adrenergic stimulation[40].

An intriguing aspect of cardiac aging is that, despite a decrease in the intrinsic heart rate, the basal heart rate of the elders remains the same of that of the adult population[10]. The stability of basal heart

rate is thought to be associated with an increased sympathetic tone. Under this hypothesis therefore the sympathetic-to-parasympathetic ratio must increase in advanced age in order to preserve the mean basal heart rate despite reduced intrinsic mechanisms. In this respect it should be mentioned that the heart-rate variability is mainly determined by the vagal activity. Several works reported a decreased heart rate variability during aging in agreement with the expected increase in the sympathetic-to-parasympathetic ratio; a very important point that must indeed be considered is that this ratio increase leads to a higher risk of morbidity and mortality.

The accepted hypothesis for the increase of the sympathetic system is therefore a compensatory mechanism necessary for the preservation of a stable basal heart rate in the elders, and a consequence of this event is the associated increase in the development of SND.

However, there is ample evidence that sympathetic tone increase during ageing is not limited to the heart and indeed occurs in many parts of the body. In particular, it has been found that there is a generalized increase of noradrenaline release and a higher concentration in plasma[41]. It is therefore possible that the increase in the sympathetic activity is not a simple homeostatic control of the aging heart rate, but may be part of a more complex systemic condition.

AIMS

The incidence of morbidity and mortality of cardiovascular diseases is becoming a major social problem due to the increase of the elderly population and of the average life expectancy; for this reason there is a raising interest in the pathophysiological mechanisms at the basis of cardiac aging.

Data in the literature highlight the evidence that the intrinsic heart rate declines during aging, while such a change is not observed in the basal heart rate, which instead remains the same. A comprehensive view of the physiological events underlying these observations is still missing, however a major hypothesis proposes that the sympathetic system increases its influence during aging to maintain unchanged the basal heart rate. The key point of this project is therefore to elucidate the cellular and molecular mechanisms that cause the reduction of the intrinsic heart rate without reducing the basal heart rate by investigating the nature of age-dependent changes of pacemaker activity in freely-moving mice and in murine sinoatrial node cells.

RESULTS

In order to better understand the mechanisms at the basis of cardiac pacemaker aging we started with a set of experiments to verify the presence also in our study model of a stable basal heart rate and a decreased intrinsic heart rate.

First of all we recorded the ECGs of 10 young (4month old) and 9 old (18-month old) freely-moving mice for six consecutive days both in light and dark conditions.

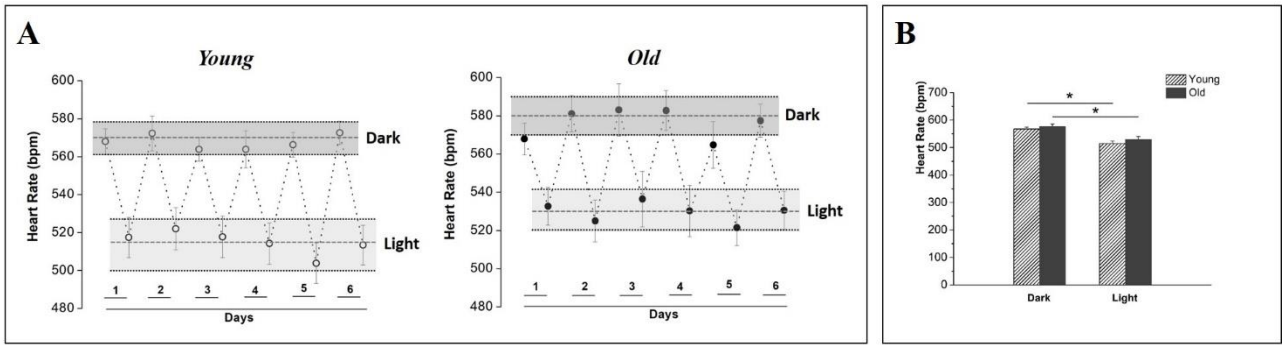

Figure 1. Basal HR does not change between young and old mice. (**A**) Time courses of young (left) and old (right) mice HR recorded for six consecutive days. Each point represents the mean HR of the dark/light period in each day. (**B**) Bar-graph of the mean HRs of all six days in the dark and in the light. n=10 (young) and n=9 (old). * P<0.01, two-way Anova.

Figure 1A shows the time courses of young (left) and old (right) animals heart rate. This type of graph highlights the difference in the heart rate recorded in the dark and in the light; the rate increases during the night and decreases during the day; this trend is similar between the two groups of animals and reflects the circadian rhythm of the mice, that are active during the dark phase of the day. The HRs recorded during the light and the dark period have been averaged and plotted in a bar-graph (**Figure 1B**). This graph shows that there are no differences between the two groups of animals. In general the basal heart rate does not change with aging: the heart rates recorded in the elderly in the dark or in the light are similar to those recorded in young mice (dark young vs old: 567.2±6.6 vs 576.1±9.9, respectively; light young vs old: 514.7±9.5 vs 529.34±10.6, respectively). The bar-graph confirms the difference of the HRs in the two different periods of the day. The HRs is significantly higher during the dark period both in young and old animals.

We then move on to evaluate how the intrinsic heart rate changes with aging. The intrinsic heart rate *in-vivo* can be measured by blocking the autonomic receptors with an i.p. injection of appropriate drugs; since we planned to use this experimental approach, we first performed a control experiment to evaluate the perturbing effects of animal manipulation and injection on heart rate. We therefore verified the injection of a saline solution in all the animals of the study and we recorded

ECGs two hours before and after the injection. This procedure allowed to set the experimental control conditions.

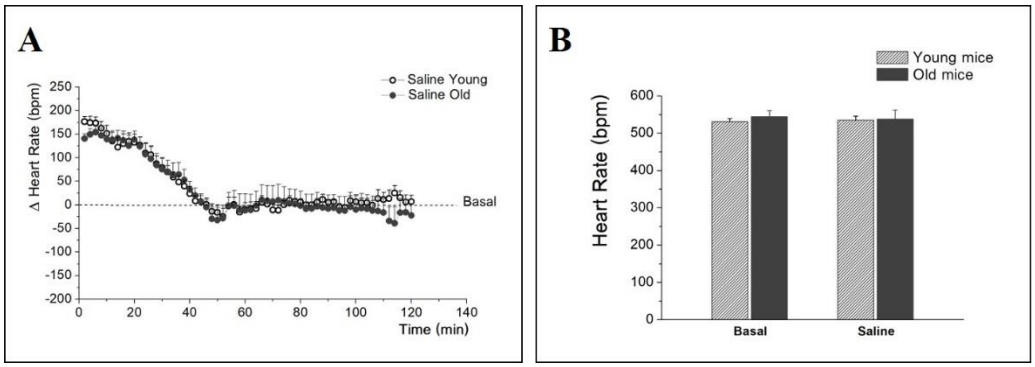

Figure 2. The injection of a saline solution does not change HR. (**A**) Time courses of ΔHR in young (empty circles) and old (full circles) mice after the injection of a saline solution. ΔHR is calculated as the difference between the HR recorded in the presence of the saline solution and the mean value of basal HR recorded the two hours immediately before the injection. (**B**) Bar-graph showing the mean HRs. For the basal value the HR recorded in the two hours before the injection was averaged; for the HR in the presence of the saline solution the mean of the second hour after the injection was plotted. n=9 (young) and n=8 (old).

The time courses of the HR (**Figure 2A**) recorded after the injection of a saline solution show an immediate increase of the HR, that returns to the basal level in about 50 minutes, and this behavior is identical in both young and old animals. The initial increase of the HR represents the stress caused by manipulation and injection. Based on these results we therefore decided to carry out all the analysis of ECGs during the second hour after the injection, when the HR has reached a steady-state and the influence of the manipulation has disappeared as can be observed in **Figure 2A** where the heart rates have values comparable to the basal ones. In the bar-graph (**Figure 2B**) the basal HRs (0 level) represent the average of the HRs of the 2 hours before the injection and it is not different from the one recorded after the injection of a saline solution at the steady state.

This type of experimental protocol represents the control for all the following experiments that required i.p. injection.

After this control experiment we recorded the intrinsic heart rate in the presence of pharmacological denervation of the autonomic system. A complete block of the autonomic nervous system was obtained by a combined injection of Atenolol (1 mg/kg) and Scopolamine (0.1 mg/kg), a β-blocker and a muscarinic receptor blocker, respectively.

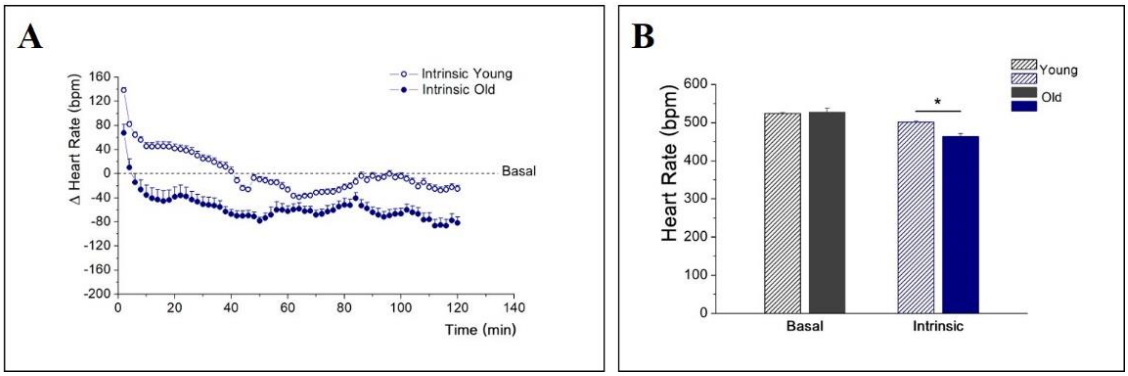

Figure 3. Intrinsic heart rate decreases with aging. (**A**) Time courses of the intrinsic heart rate of young (empty circles) and old (full circles) mice. ΔHR is calculated as the difference between the intrinsic HR and the mean value of basal HR recorded the two hours immediately before the injection. (**B**) Bar-graph showing the mean HRs. The basal bars correspond to the mean HRs recorded in the two hours before the injection; for the intrinsic HR the mean of the second hour after the injection was plotted. n=9 (young) and n=7 (old). *P<0.05, Student's T-test.

The time courses of the intrinsic heart rates identified a lower rate in old than in young animals (**Figure 3A**); the mean steady-state intrinsic heart rates (IHR) are plotted in the bar-graph (**Figure 3B**) and confirmed that aging significantly affects (decreases) this parameter. In the bar-graph, the basal heart rate recorded two hours before the injection of autonomic blockers is also reported to better illustrate that basal heart rate does not change during aging while intrinsic heart rate decreases.

In order to understand the reason of the decrease of the intrinsic heart rate we decided to proceed by characterizing one of the main current that sustains cardiac pacemaking: the *funny* current.

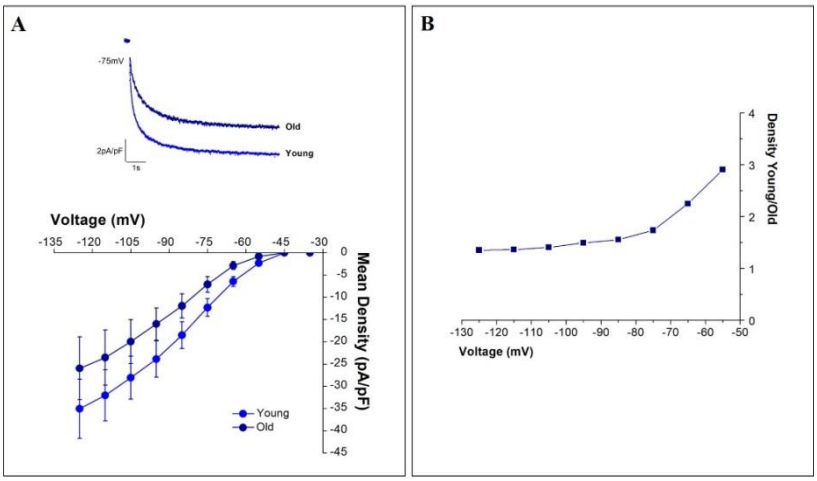

Figure 4. *Funny* current density decreases with aging. (**A**) Top, sample traces of I_f current density recorded at -75mV from young (light blue) and old (dark blue) mice. Bottom, mean *funny* current densities at different voltages recorded in young and old mice. n=17 (young); n=9 (old). (**B**) Ratio between I_f current density of young and old animals at different recording voltages.

Our data clearly show that aging reduces the I_f current density. Mean steady-state I_f current densities were measured at different voltages (**Figure 4A**, bottom) and the graph clearly show a reduction of the current density, significant at diastolic potentials (-45 mV, -55 mV, -65 mV). Sample traces recorded at -75 mV s are also shown (**Figure 4A**, top). To evaluate the entity of reduction at each potential, we divided each point of the mean current density of young mice by the corresponding values recorded in old mice (**Figure 4B**).

This graph highlights a different reduction of the current density at different voltages: at the more hyperpolarized potentials the difference is constant, while at more physiological potentials (from -75 mV to -55 mV) the entity of reduction increases. This type of graph highlights the fact that at negative voltages (i.e. where the conductance is somewhat maximal) the decrease in density is stable, while at more positive voltages a clear voltage dependent effect appears possibly due to differences in the activation curves between the two groups of animals. We then evaluated the voltage dependence of the I_f by constructing the activation curves shown in **Figure 5**.

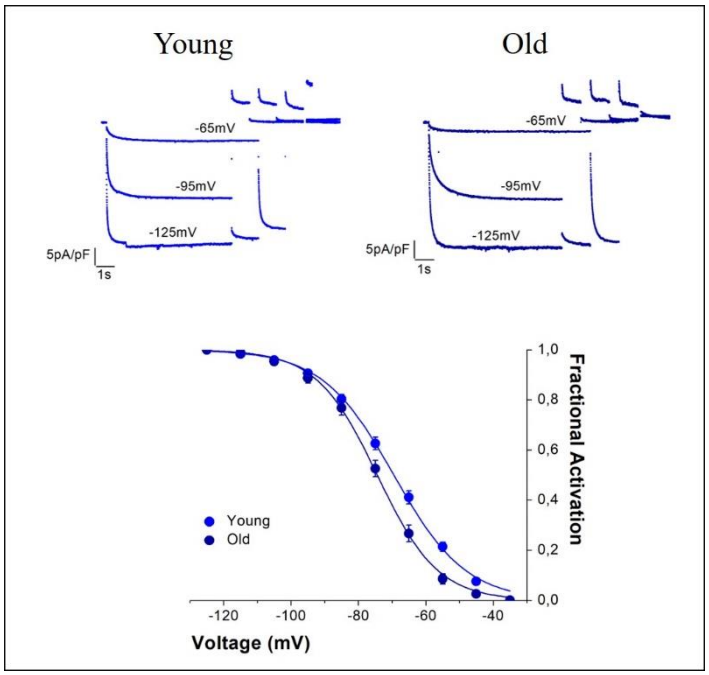

Figure 5. Aging causes a leftward shift of the I_f activation curve. Top, sample traces of the activation curve of young (left) and old (right) mice. Three of the ten pulses of the protocol are shown in the figure (-65mV, -95mV, -125mV). Bottom, mean activation curves in young and old mice. $V_{1/2}$ young vs old: -69.5±1.1 vs -74.4±1.1; P<0.01, Student's T-test. n=17 (young); n=9 (old).

In the top panels of the figure sample traces recorded by applying the activation protocol are shown. The mean activation curves (bottom) show a significant difference in the half-activation values between the two groups ($V_{1/2}$ young vs old: -69.5±1.1 vs -74.4±1.1, respectively); in particular, there is a leftward shift of the activation curve of old animals compared to the young. Furthermore,

there is a difference in the slope of the curves that causes a different shift at different potentials; in particular the shift increases at more depolarized potential, which is partially the explanation of the results on the current density described in **Figure 4**.

These differences in the I_f current characteristics reflect the reduction of intrinsic heart rate recorded *in-vivo*.

To better understand the reason of the reduction of the intrinsic heart rate but not of the basal one, we performed other *in-vivo* experiments to evaluate the influence of each branch of the autonomic system. Basal heart rate is in fact generated by the intrinsic heart rate modified by the sympathetic and parasympathetic control modulation.

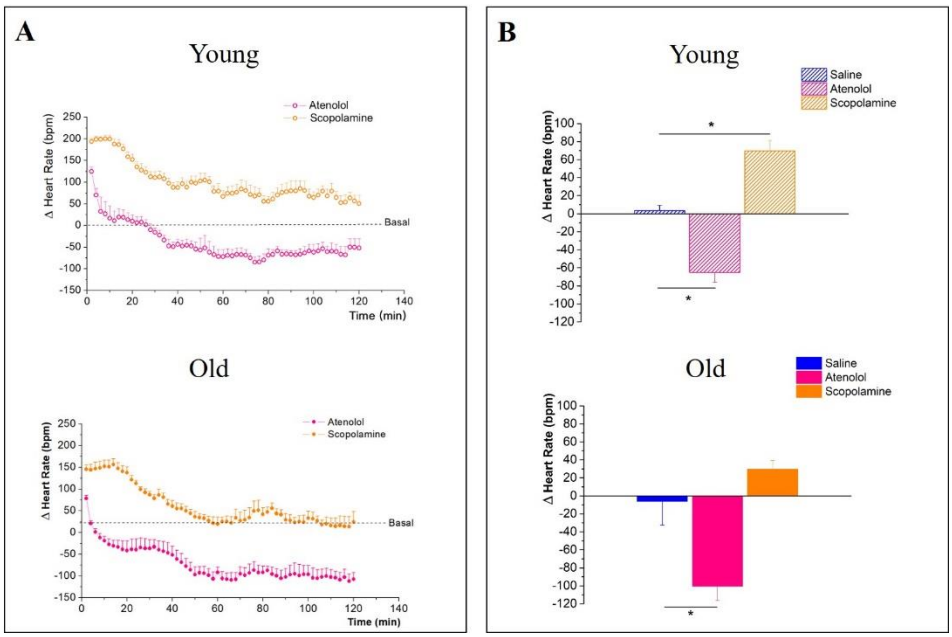

Figure 6. The sympatho-vagal system is balanced in the young and unbalanced in the old mice. (**A**) Time courses of ΔHR in young (top) and old (bottom) mice after the injection of Atenolol (pink) or Scopolamine (orange). ΔHR is calculated as the difference between the HR recorded after the injection of the substance of interest and the mean value of basal HR recorded the two hours immediately before the injection. (**B**) Mean ΔHRs plotted in bar-graphs show the contribution of the sympathetic (pink) or parasympathetic (orange) systems. The ΔHR of saline are also reported as comparison. Atenolol: n=9 (young), n=7 (old); Scopolamine: n=9 (young), n=8 (old). *P<0.05, one-way Anova.

We injected Atenolol (1 mg/kg) or Scopolamine (0.1 mg/kg) to block either the sympathetic or parasympathetic system, respectively. The time courses of young and old mice presented in **Figure 6A** show a similar decrease of the heart rate in the presence of atenolol. On the other hand, a different observation can be made between the two groups in the presence of scopolamine. For young animals the entity of increase in the heart rate in the presence of scopolamine is substantial

while it is minimal in the elders. This different behavior suggests a shift in the sympatho-vagal balance system towards the sympathetic control.

The modules of the mean ΔHR plotted in the bar-graphs (**Figure 6B**) reflect sympathetic activity and the parasympathetic activity; these modules are not different in the young animals (65±11 and 70±12, respectively), while they are significantly different in the old animals (sympathetic influence: 100±16; parasympathetic influence: 30±10), with a prevalence of the sympathetic system.

To further evaluate the difference in the symaptho-vagal control exerted in young and in old animals we also used a different type of experimental approach, the Heart Rate Variability (HRV) (**Figure 7**). The overall variability was assessed by the analysis of the total power. This analysis highlighted a significant decrease of HRV with aging (**Figure 7A**). As previously mentioned, a decrease in the total power of variability is an index which grossly indicates a decreased influence of the parasympathetic modulation of rate or an increase in the sympathetic control.

The specific influence of the two branches of the autonomic nervous system was then evaluated with the measure of the high and low frequencies. High frequency (HF) reflects the activity of acetylcholine, and so that of parasympathetic system; the activity of the sympathetic system is instead identified as the ratio between low and high frequency (LF/HF).

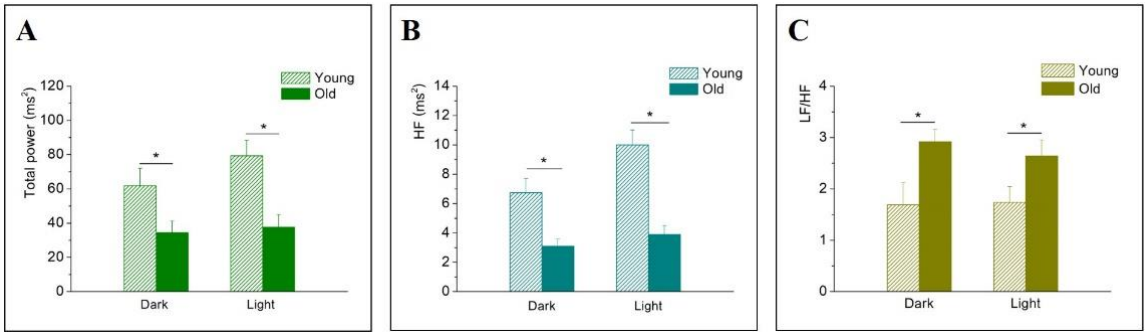

Figure 7. Heart rate variability decreases with aging. (**A**) Analysis of total power on young and old mice. (**B**) High frequency values plotted in a bar-graph. (**C**) Ratio between low frequency and high frequency. n=10 (young) and n=9 (old). * P<0.01, two-way Anova.

The HF component of the variability decreases with aging, underling a reduction in the parasympathetic influence (**Figure 7B**), and the LF/HF ratio significantly increases with aging, confirming a shift of the sympatho-vagal balance towards a sympathetic prevalence in the elders (**Figure 7C**).

We next proceed to evaluate the maximum and minimum heart rate using agonists of sympathetic and parasympathetic system, respectively.

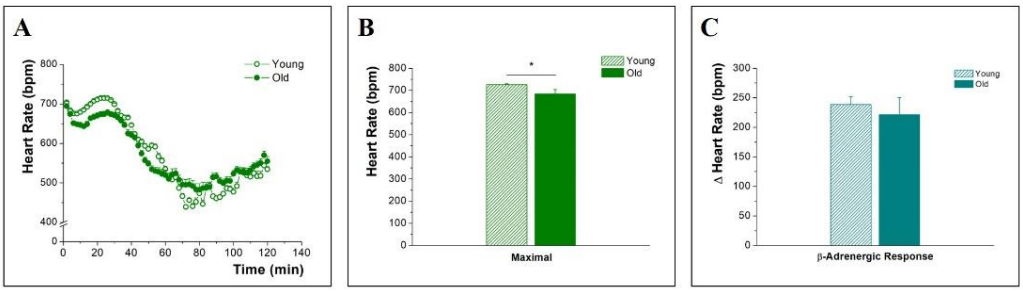

	INTRINSIC HR	MAXIMAL HR	ADRENERGIC RESPONSE
YOUNG	487,7±12	726,2±3,8	238,4±13,3
OLD	462,4±9,7	683,9±20,4	221,4±28,9

Figure 8. Maximal heart rate decreases with aging while adrenergic response does not. (**A**) Time courses of heart rate after the injection of a saturating dose of Isoproterenol (0.2 mg/kg) in young (empty circles) and old (full circles) mice. (**B**) Mean maximal heart rate calculated as the maximum value of heart rate at about 20 minutes after injection. (**C**) β-adrenergic response calculated as the difference between maximal and intrinsic heart rate. Mean values used to calculate the adrenergic response of each group are reported in the table. The adrenergic response value is the mean of the adrenergic response calculated in single animals. n=8 (young) and n=7 (old). *P<0.05, Student's T-test.

Maximum heart rate was obtained using a saturating dose of Isoproterenol (0.2 mg/kg) and it was calculated as the higher value of heart rate reach about 20 minutes after the injection. The time courses shown in Figure 8A suggest a decrease in the maximal heart rate in old mice compared to the young, and this impression was confirmed by the statistical analysis carried out on mean maximal heart rates (Figure 8B). In order to understand if this difference in the maximal heart rate was correlated to a difference in the ability to respond to adrenergic stimuli, we calculated the β-adrenergic response as the difference between the maximal heart rate and the intrinsic heart rate. ΔHRs corresponding to the β-adrenergic responses are shown in Figure 8C and all the values used are reported in the table. The statistical analysis demonstrates that there is no difference between the two groups. This evidence is of extreme interest because it suggests that no β-desensitization occurs in our ageing model.

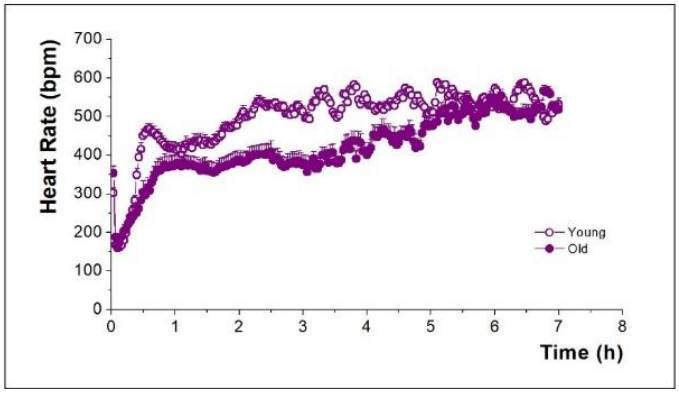

Figure 9. The maximal muscarinic response seems to be similar between young and old animals, while the recovery seems different. Time courses of young (empty circles) and old mice (full circles) after the injection of Carbachol (0.5 mg/kg), a muscarinic agonist. n=8 (young) and n=6 (old).

We also made a similar study on the muscarinic response and preliminary data are shown in **Figure 9**. The muscarinic response was evaluated with the injection of a saturating dose of Carbachol (0.5 mg/kg). The decrease of heart rate immediately after the injection seems to be similar between the two groups. However the trend of recovery from the muscarinic agonist seems to be different, with a slower recovery in the old animals. This evidence is extremely puzzling and needs to be better characterized with future experiments.

DISCUSSION

Cardiac aging is an intricate field: several functional and anatomical changes characterize the heart decline during aging. If we consider the electrical function, there is a strong tissue remodeling which impairs the cells of all the cardiac conduction system. These changes make the aged heart more susceptible to diseases.

It is demonstrated that the incidence of morbidity and mortality associated with cardiovascular diseases increases exponentially in the elderly population due to both the increasing number of old people and the average life expectancy. It has been predicted that by 2035 almost 25% of the population will be over 65 years old[6].

Among the age-dependent cardiac diseases, sinus node dysfunctions have a primary role. Age-related SAN dysfunctions may explain the development of cardiac complications that require pacemaker implantation in the elders.

Since the mechanisms of the age-associated physiological cardiac changes are yet to be fully understood and the causes of the related diseases are still uncertain, therefore there is a high interest in this topic.

In our laboratory, we study the mechanisms at the basis of cardiac pacemaker in physiological and pathological conditions.

Given the importance of the problem of cardiac aging we started this project with the intent of investigating the nature of age-dependent changes of pacemaker activity using young and old freely-moving mice and single sinoatrial node cells.

The first experiments were carried out to confirm the evidence already described in the literature. **Figure 1** demonstrated that basal heart rate does not change between young and old mice, as it was previously described both in mice and humans[8,9,39,42]. The other important result is shown in **Figure 3**: while basal heart rate does not change with aging, intrinsic heart rate does, and in particular it decreases in the older animals. This is another result in agreement with the literature. These two findings gave rise to a series of questions that were analyzed in the following experiments. In this study (described in the results) we focused our attention on the physiological events responsible for the reduction of the intrinsic heart rate and for the intriguing issue of the maintenance of the basal heart rate.

The reduction of the intrinsic heart rate is associated with a general deterioration of the sinoatrial node, which causes a reduction in the impulse conduction, in the number of cells, and in the reduction of excitability of single SAN cells. We have therefore studied these aspects by means of electrophysiological experiments on single SAN cells isolated from young and old mice. There is ample evidence in the literature that the firing rate of SAN cells isolated from old animals is slower

when compared to the firing of young SAN cells[39]. In addition, the rate reduction is primarily caused by the decrease in the slope of the early diastolic depolarization. Since this phase is sustained by the funny current we further investigated this aspect by evaluating the characteristics of this current. We found changes in different parameters of the current (**Figures 4-5**). There is a reduction in the current density and a leftward shift of the activation curve, a parameter that describes the voltage dependence of the current. These findings are therefore perfectly compatible with the reduction of the intrinsic heart rate observed with ageing. The analysis of the voltage dependence of the I_f current also revealed another interesting difference between the two groups: the slope of the activation curve. This parameter, in general, reflects the number of gating charges displaced during channel activation, and the steeper is the curve, the stronger is the voltage dependence. The difference in the slopes could be explained in various way. One of the simplest is a partial switch in the HCN isoforms composition that assemble the I_f channels. Regarding this aspect, it has been demonstrated that I_f current passing through different HCN channels isoforms has different kinetics and $V_{1/2}$ ($V_{1/2}$ HCN2: -92 mV; $V_{1/2}$ HCN4: -81mV)[28].

Since old animals have a steeper slope than young animals and a more negative $V_{1/2}$, it could be that old animals have a higher ratio between HCN2 and HCN4 channels.

In literature there are very few works on HCN channels expression with aging[43]. From these researches it seems that there is a general reduction of HCN channels expression, in agreement with the reduction of I_f current. Furthermore it seems that with aging there is an increase of HCN2/HCN4 ratio[43], which could explain the difference in the kinetics of I_f activation and in the $V_{1/2}$ between young and old mice.

The other target of my Ph.D. project was to investigate the reason of the maintenance of the basal heart rate with aging despite a reduction of the intrinsic heart rate.

Since the main aspect that differentiates the basal heart rate from the intrinsic heart rate is the autonomic nervous system influence, we investigate if the autonomic control could be the key for the explanation of this compensation of the reduction of intrinsic heart rate. The experiments performed *in-vivo* with the injection of muscarinic or adrenergic blockers show that there is a modification of the sympatho-vagal balance with aging (**Figure 6**); this observation was further confirmed by using the Heart Rate Variability analysis of the total power, before, and LF/HF ratio, then (**Figure 7A** and **7C**). Both these results highlight the prevalence of the sympathetic activity in old mice compared to the young animals. According to these data, it is possible to conclude that the mechanism behind the preservation of the basal heart rate during aging appears to be an augmentation of the sympathetic nervous system activity that compensates for the age-dependent decline in intrinsic heart rate. It is known that proper balance between sympathetic and

parasympathetic system is necessary for proper functioning of the cardiovascular system[44]. An unbalance of the system can lead to pathological states. In particular, a decrease of HRV and an increase in sympathetic tone are triggering factors for arrhythmic conditions, which is typically observed in the elderly. Based on this line of reasoning the higher sympathetic tone observed in the elderly, which is necessary for compensating the reduction of intrinsic heart rate, is by itself a mechanism that exposes the entire system to an unstable and risky condition for arrhythmic states. Furthermore this compensatory system is absent in several other conditions that cause the reduction of SAN rate. Among these, mutations causing congenital sinus bradycardia are not compensated by an increased adrenergic tone, with an evident bradycardia as phenotype[45]. It seems that a compensation of the reduction of the intrinsic is therefore not so necessary, since bradycardia is not a risky condition. Moreover, this type of compensation is pro-arrhythmic. Taken together these two considerations open the possibility of the existence of a different view to interpret the reduction of intrinsic heart rate but not of the basal one.

It has been demonstrated that the age-dependent increased tone of the sympathetic nervous system is a physiological condition that could be caused by a general increase of the subcortical central nervous system sympathetic drive[41]. However, the increase of the sympathetic activity appears to be region specific and it is measured by the spillover of noradrenaline from tissues to plasma. Cardiac plasma spillover is higher in the elders.

Considering that the sympathetic tone is found to be increased also in other districts (the gut and the skeletal muscle), the evidence supports the view that human aging is associated with a net activation of the sympathetic nervous system.

An increase of the sympathetic activity on the cardiovascular system leads to a tachycardic condition, that is risky, especially in the aged people. For these reasons we hypothesize that the reduction of the intrinsic heart rate is the compensatory mechanism that restores the basal heart rate, and not the cause of the increase in the sympathetic activity. In support of this new hypothesis there is the evidence that the physiological electrical remodeling of the SAN is a mechanism of adaptation to different conditions, such as exercise. This indicates that the expression of sinus node channels can be modulated in order to respond to external stimuli. Aging and exercise, moreover, have a common mechanism that could be the cause of the reduction of HCN channels expression: an increased sympathetic activity.

Further experiments that simply induce an increase of adrenergic response (chronic Isoproterenol injection) are necessary to verify the hypothesis of the reduction of the intrinsic heart rate as a compensatory mechanism for the sympathetic augmentation.

Another important aspect of cardiac aging that we evaluated in this project is the reduction of the maximum heart rate. In the literature the reduction of maximal heart rate is associated with both the reduction of intrinsic heart rate (confirmed by our data) and a β-desensitization[40]. However, to date our data do not show a significant decrease of the β-adrenergic response. We will increase the number of animals to verify this aspect.

We finally evaluated the effect of muscarinic agonists on heart rate in young and old mice. These are preliminary data (**Figure 9**). There are almost two aspects that emerge from this trend. The first one is that there is a strong decrease of the heart rate immediately after the injection of Carbachol; the entity of this decrease is very similar between young and old mice, which means that the minimum value of heart rate they can reach is the same. The second aspect is that there is a different trend in the recovery from the effect of the substance. In particular it seems that old mice have more difficulties to remove Carbachol. Further experiments will clarify these different actions in the two groups.

At the end of this discussion I want to spend some words about the validity of mice as aging models. Mouse could be considered a bad model since, for example, in the resting state it has no vagal prevalence, as happens in humans, and the mean basal heart rate of mice is really higher than that of humans. However, the results obtained in this study from mice are totally comparable to the ones from humans: 1) the basal heart rate is preserved and 2) the intrinsic heart rate, together with the maximum heart rate, declines with age; 3) the overall HRV decreases and 4) the sympathetic contribution augments in elder animals. Taking into account these considerations, we can state that mouse represents a good model for cardiac aging.

Mode of action of the Traditional Chinese Medicine drug TMYX on pacemaker activity in freely-moving mice and in isolated SAN cells

INTRODUCTION

The discovery of the I_f current has opened the search for agents able to specifically block this current and thus able to reduce heart rate by reducing the diastolic depolarization slope. Given the clinical relevance, various "pure bradycardic agents" have been developed in the last few years[46]. These drugs are potentially able to reduce the SAN pacemaker activity without the inotropic side effects typical of drugs currently used, such as Ca^{2+} antagonists or β-blockers[47,48]. However, some of these drugs also affect other channels such as Ca^{2+} and K^+ channels and are therefore potentially pro-arrhythmic. To date, Ivabradine is the only pure bradycardic agent without important side effects and it is largely used for the clinical treatment of angina pectoris, ischemia and heart failure. Given these premises, the interest in the search for novel pure bradycardic agents has acquired a great importance in pharmacology.

In this contest in the recent years there is an increased interest for compounds derived from the Traditional Chinese Medicine. Tongmai Yangxin (TMYX) is a TCM drug able to modulate cardiac rate and is largely used in China for the treatment of cardiac diseases, such as Left Ventricular Premature Beats (LVPB), Heart Failure (HF), and Coronary Artery Disease (CAD). This drug is a mixture of different compounds, including flavonoids, coumarins, iridoid glycosides, saponins and lignans.

STATE OF ART

Few years ago our laboratory started an electrophysiological study on the TMYX, since the mechanism of action of this compound was unknown; a series of *in-vitro* electrophysiological experiment on single sinoatrial node cells isolated from rabbit heart were therefore performed.

The results obtained in the first experiments are summarized below:

1) TMYX induces a dose-dependent rate slowing of the spontaneous activity (action potentials) of rabbit single pacemaker SAN cells, and the slowing is mainly due to a decrease of the slope of the diastolic depolarization. This effect is fully reversible at all concentrations tested. (**Figure 1**).

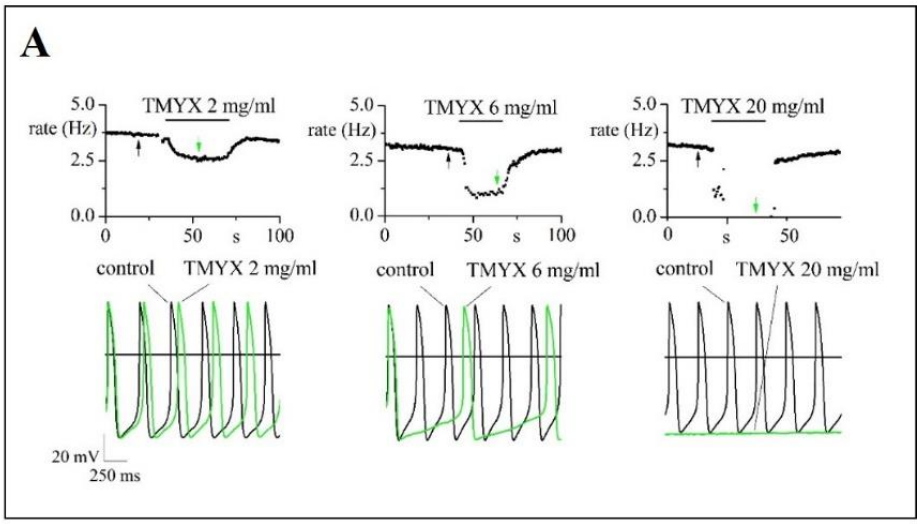

B

TMYX	n	Rate					
		Ctrl (Hz)		TMYX (Hz)		% Reduction	
		Mean	S.E.M.	Mean	S.E.M.	Mean	S.E.M.
0.2 mg/ml	7	3.34	0.28	3.21	0.27	-3.96 *	0.55
0.6 mg/ml	6	3.59	0.18	3.32	0.18	-7.58 *	1.17
2 mg/ml	23	3.50	0.12	2.67	0.09	-23.55 *	1.20
6 mg/ml	6	3.17	0.19	01.52	0.16	-51.64 *	5.02
20 mg/ml	7	2.94	0.22	0	0	-100 *	0
60 mg/ml	3	2.25	0.25	0	0	-100 *	0

Figure 1. TMYX reduces AP rate of rabbit single SAN cells. (**A**) Examples of time courses of the rate (top) and AP traces (bottom) in control conditions and after perfusion of different concentrations of TMYX. (**B**) Mean of rate in control and after TMYX perfusion. *P<0.05, Student's T-test.

2) TMYX induces the decrease of the I_f current at -65 mV and an increase at -125 mV (**Figure 2A**); furthermore it shifts the half-activation of the mean activation curve to the left (**Figure 2B**). The mean steady-state curve (**Figure 2D**) demonstrates that at potentials more positive than -80 mV the contribution of the leftward shift of the activation curve induced by TMYX prevails over the conductance increase, and the overall effect is a decrease of current.

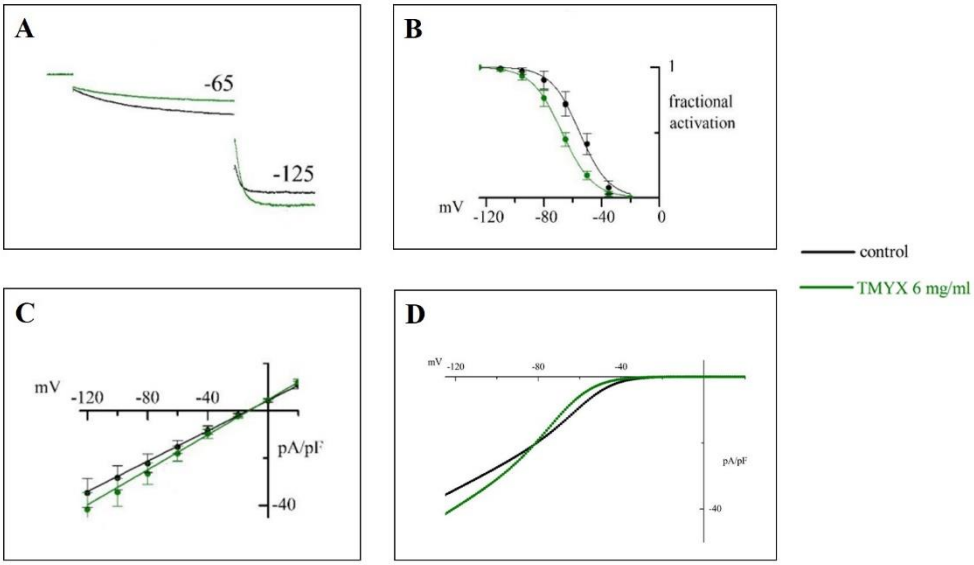

Figure 2. TMYX reduces the I_f current availability. (**A**) Two-step protocol used to investigate the effect of TMYX 6 mg/ml on the I_f current. (**B**) Mean activation curves in control (black) and during perfusion of TMYX 6 mg/ml (green); (n=6, $P < 0.05$, paired sample t-test). (**C**) Mean current-voltage relationships in control and with TMYX (same meaning of colors); (n=5, $P < 0.05$, paired sample t-test). (**D**) Mean steady-state curve in control and in presence of TMYX 6 mg/ml obtained by multiplying the activation curves by the fully-activated IV relationship.

These experiments therefore highlight the fact that at pacemaker potentials TMYX reduces the I_f current and SAN cell firing rate.

AIMS

Natural compounds used in Traditional Chinese Medicine (TCM) have a long history of proven therapeutic efficacy and this aspect has now been amply acknowledged also by western medicine.

Pharmacological reduction of heart rate (HR) is often necessary to treat cardiomyopathies and administration of β-blockers is often the primary approach. Unfortunately β-blockers have undesired and frequently intolerable side-effects; for this reason the search for more specific molecules is considered a priority in the cardiac biomedical field.

The aim of this project consists in the identification of the mechanisms of action of Tongmai Yangxin (TMYX), a TCM drugs currently used in China for the treatment of cardiac arrhythmias, using modern technologies.

Since previous data from the lab where I carried out my Ph.D. thesis project demonstrate that the TCM drug TMYX is a potent modulator of pacemaker rate I reasoned that it would important to investigate more in detail the mechanism of action of this drug. Understanding this aspect is extremely important for the clinical and therapeutic implications for clinician who prescribe this drug.

To this aim *in-vivo* experiments were performed in freely-moving mice to evaluate the systemic effect of the drug, and *in-vitro* experiments were carried out in single SAN cells to better understand the mode of action of TMYX.

RESULTS

In-vitro experiments:

The *in-vitro* experiments performed in our laboratory (see *State of art* in the introduction section) demonstrated that the main effect induced by TMYX on SAN cells consists in the shift of the I_f activation curve to more negative voltages. Interestingly and importantly, the same mechanism of action is also applied by the autonomic system to control the I_f availability and to induce heart rate increase or decrease. A shift toward more negative voltages is generated by low cAMP availability, a mechanism used by the cholinergic M2 muscarinic receptor activation, while a shift towards more positive voltages is generated by high cAMP availability, a mechanism used by sympathetic β-adrenergic receptor activation. My data on TMYX action therefore ultimately resemble those of a cholinergic/parasympathetic modulation.

I thus planned an experiment to verify whether TMYX (6 mg/ml) maintains its ability to inhibit the I_f current after the current is maximally reduced by a saturating concentration (1 μM) of ACh. The I_f current was elicited by a train of steps to -65 mV (from a holding potential of -35 mV) and the cell was subsequently exposed to TMYX alone or to TMYX and ACh (1 μM). The time course of the I_f current recorded at -65 mV in a SAN cell exposed to this protocol is plotted in **Figure 1A** and sample current traces are shown in **Figure 1B**.

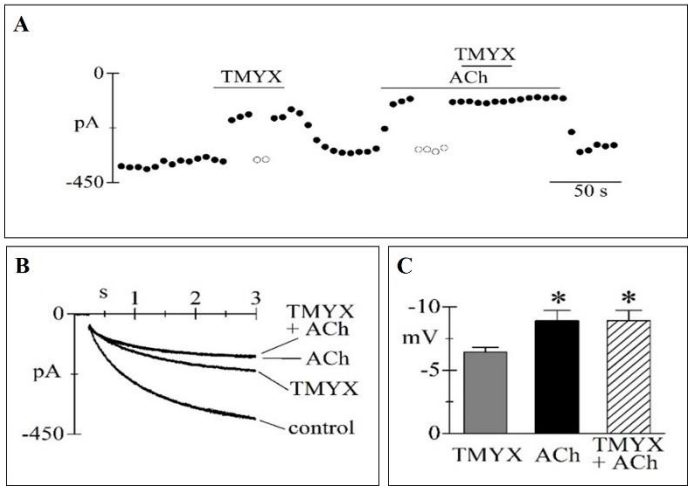

Figure 1. TMYX and ACh share a common mechanism. (**A**) Sample time course of the I_f current amplitude during steps to -65 mV upon perfusion of TMYX 6 mg/ml and ACh 1 μM, applied either separately or in combination. Empty dots represent manual corrections of the applied voltage, used to measure the shift. (**B**) Sample I_f current traces in control and in the presence of TMYX 6 mg/ml, ACh 1μM, and TMYX 6 mg/ml + ACh 1 μM. (**C**) Bar-graph of the shifts induced by TMYX 6 mg/ml, ACh 1 μM, TMYX 6 mg/ml + ACh 1 μM. n=6, *P < 0.05 versus TMYX, One-way ANOVA, Fisher test.

Separate exposures to TMYX and ACh caused a current reduction that was quantified as a shift in the activation curve (Figure 1). TMYX induced a mean shift of -6.4 ± 0.4 mV while ACh (1 µM) induced a mean shift of -8.9 ± 0.8 mV (n=6 cells). The difference in the mean shifts was statistically significant, reflecting the fact that at the concentrations used ACh had a significantly stronger effect. More interestingly, when TMYX was perfused in the presence of ACh, the drug could not elicit any additional effect. This experiment was carried out in 6 cells and I never observed any effect of TMYX in the presence of ACh. This evidence clearly suggests that the modulatory pathways elicited by TMYX and ACh share a common mechanism.

To address this question, I first evaluated the possibility that TMYX may act as an activator of the muscarinic receptor and to test this hypothesis I used atropine, a muscarinic receptor antagonist. While atropine was able to fully block the ACh-dependent modulation of both the I_f current and the spontaneous activity (**Figure 2A**), it did not affect the ability of TMYX to reduce I_f and AP rate (**Figure 2B**). The time courses of I_f at -65 mV and of spontaneous rate are also shown (**Figure 2C**). Bar-graphs in **Figure 2D** quantify the effects of TMYX on the I_f current (shift in mV) and on spontaneous rate (% of rate-reduction) as compared to control.

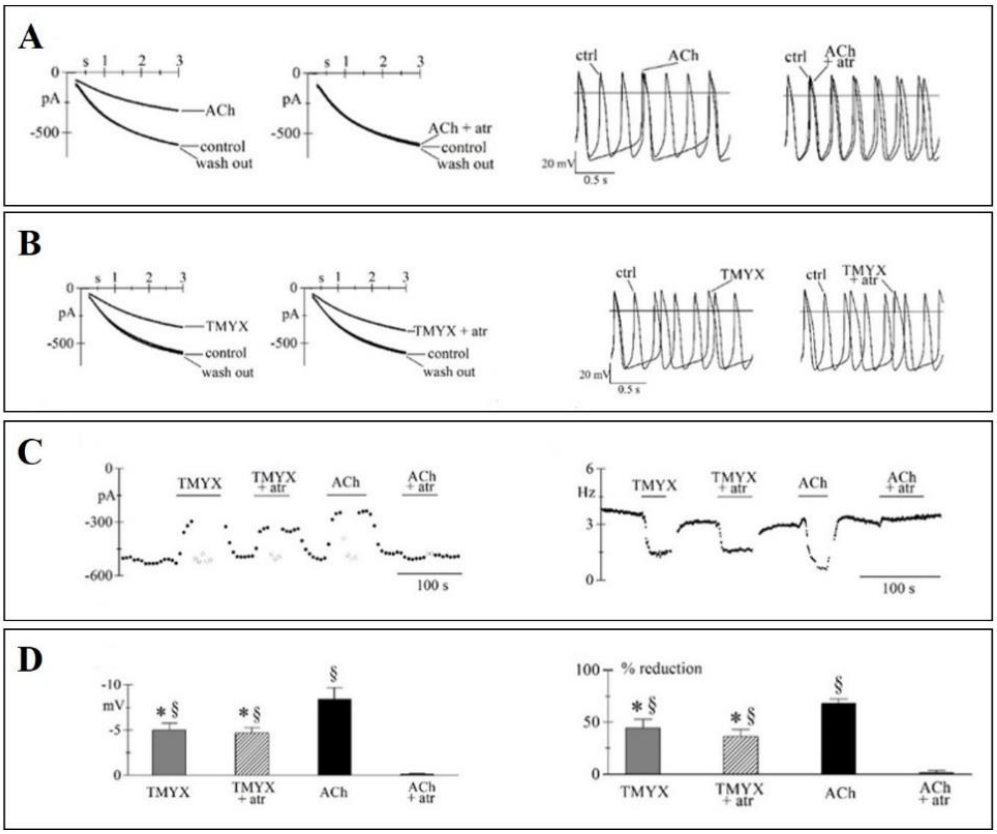

Figure 2. TMYX does not activate muscarinic receptors. (**A**) Sample traces of I_f currents during steps to -65 mV (left) and spontaneous activity (right) recorded in the presence of: ACh 1 µM or ACh 1 µM + Atropine 10 µM. (**B**) Sample traces of I_f currents during steps to -65 mV (left) and spontaneous activity (right) recorded in the presence of: TMYX 6 mg/ml or TMYX 6 mg/ml + atropine 10 µM. (**C**) Time course of the I_f current amplitude at -65 mV (left) and spontaneous activity (right) recorded in the presence of: TMYX 6 mg/ml alone or in combination with Atropine 10 µM, and subsequently of ACh 1 µM alone or in combination with Atropine 10 µM. Empty dots represent manual corrections of the applied voltage, used to measure the shift. (**D**) Bar-graphs of the mean shifts of the I_f activation curve (left) and APs rate (right) measured as shown above. *, §P<0.05, One-way ANOVA, Fisher test.

Taken together these results rule out the possibility that TMYX shifts the I_f activation curve to more negative voltages by a direct activation of M2 muscarinic receptors.

I therefore further proceeded to verify which of the signal transduction stations (downstream to the muscarinic receptor), such as Adenylyl Cyclase, Phosphodiesterase, cAMP is shared between TMYX and ACh.

A set of experiments was carried out to evaluate the effect of TMYX in the presence of the following substances: 1) forskolin, a diterpenoid able to activate the adenylyl cyclase and to raise the cAMP concentration; 2) 3-Isobutyl-1-methylxanthine (IBMX), an inhibitor of cAMP phosphodiesterases that induces an increment of cAMP level; 3) cAMP added in the recording

pipette, that can diffuse into the cell and raises the cellular concentration of cAMP. These substances were added, alone or in combination, to the pipette solution as reported in **Figure 3**. In the experiment (whole-cell patch-clamp technique) the I_f current was elicited by a train of 4 s-long steps to -65 mV from a holding potential of -35 mV. TMYX 6 mg/ml was first applied alone to test for its inhibitory effect and its effect was quantified as a shift of the activation curve; TMYX was then applied in combination with the above-mentioned drugs to test whether they were able to modify the inhibitory action of TMYX. Data reported in the bar-graph and in the table of **Figure 3** show that TMYX effect is clearly diminished when cellular cAMP content is maintained at high levels by administration of forskolin, IBMX, and cAMP in the recording pipette alone or in various types of combinations, and the effects of these substances are clearly additive.

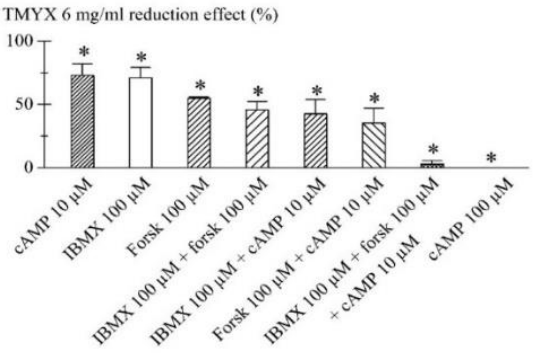

Intracellular solution	mV shift	N
Control	5.9 ± 0.3	22
cAMP 10 µM	4.2 ± 0.5 *	8
IBMX 100 µM	4.1 ± 0.5 *	6
Forskolin 100 µM	3.2 ± 0.1 *	5
IBMX 100 µM + Forskolin 100 µM	2.6 ± 0.4 *	4
IBMX 100 µM + cAMP 10 µM	2.5 ± 0.7 *	4
Forskolin 100 µM + cAMP 10 µM	2.0 ± 0.7 *	4
IBMX 100 µM + Forskolin 100 µM + cAMP 10 µM	0.2 ± 0.2 *	6
cAMP 100 µM	0 *	5

Figure 3. The enhancement of cAMP pathway reduces the TMYX action on the I_f current. Bar-graph (top) and table (bottom) showing the reduction of TMYX effect in the presence of different substances that increase intracellular cAMP. 100% represents the complete effect exerts by TMYX alone in control conditions. *P<0.05 vs control, Two sample t-test.

The most striking effect was observed in the presence of 100 µM cAMP in the pipette. At this cAMP concentration, which is considered a saturating dose, the effect of TMYX was completely abolished. These results therefore clearly indicate that the mechanism of action of TMYX is based on the reduction of cAMP. Experiments showed in **Figure 3** demonstrated also that adenylate cyclase and phosphodiesterase activity were not affected by TMYX.

We therefore investigated the effect of TMYX using the inside-out configuration in order to explore an eventual direct interaction between TMYX and HCN channels. After testing the integrity of the inside-out configuration by exposure to cAMP (10 µM) I evaluated the action of TMYX on the channel open probability, using a 60-s ramp protocol, from -35 to -145 mV (**Figure 4A**). The ramp was sufficiently slow to allow the measurement of steady-state current, throughout the voltage range investigated. Macro-patch I_f steady-state I-V relations were plotted after leakage correction (**Figure 4B**). Probability curves were then fitted with the Boltzmann equation to yield half-activation values (**Figure 4C, D**).

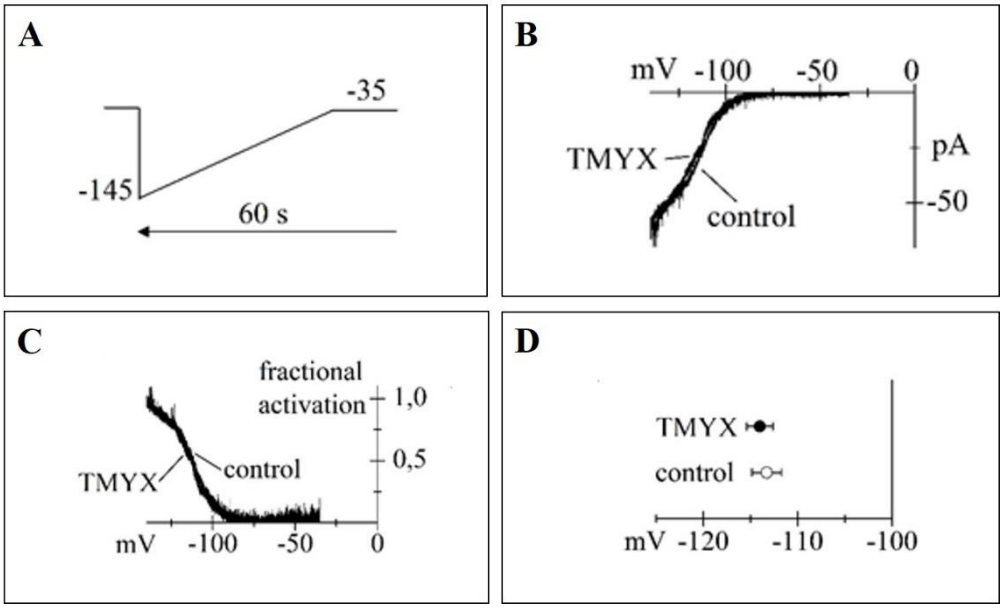

Figure 4. TMYX does not affect the probability of HCN channels opening. (**A**) Voltage ramp protocols of 60-s from -35 to -145 mV applied to inside-out patches. (**B**) Sample currents elicited in control condition and during TMYX 6 mg/ml perfusion. (**C**) Probability curves calculated as the ratio between the steady-state I-V curve and the fully activated relation. (**D**) Curve fitting by the Boltzmann equation yielded mean $V_{1/2}$ values in control condition and in the presence of TMYX 6 mg/ml, respectively (n=6).

Representative activation curves (**Figure 4C**) show no difference between control condition and during TMYX 6 mg/ml perfusion, and the analysis yielded mean $V_{1/2}$ values of -113.3 ± 1.6 mV and -114.0 ± 1.4 mV, respectively (**Figure 4D**). These data clearly demonstrate that TMYX has no direct effect on pacemaker channels. We then excluded that TMYX acts on the channel by blocking its accessibility pathway.

The absence of a direct blocking effect on the HCN channels was also verified using train of hyperpolarizing steps from -35 to -105mV every 6-s to evoke the I_f current in inside-out configuration. Sample current traces and the relative time-course are shown in **Figure 5**. It is

evident that, while cAMP alone (10 µM) can increase the size of the current, the perfusion with TMYX 6 mg/ml does not alter the amplitude of current.

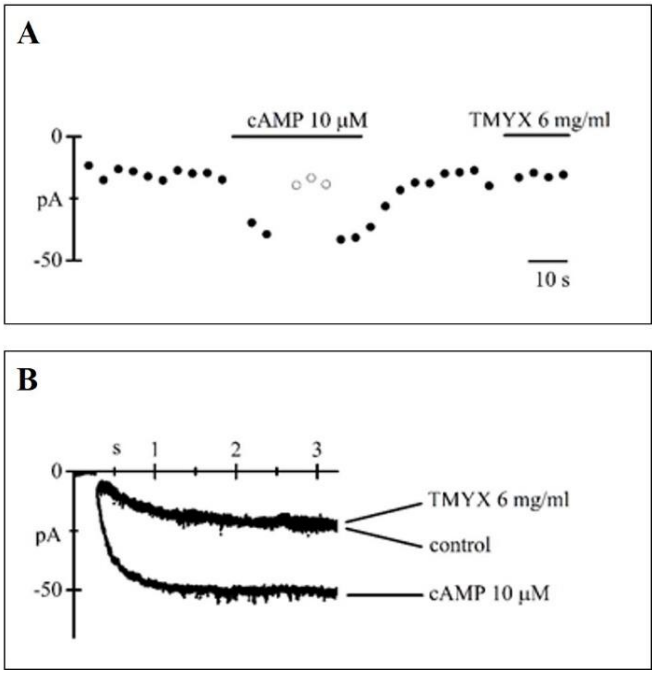

Figure 5. TMYX does not reduce the I_f current in inside-out configuration. (**A**) Sample time course of the I_f current amplitude during steps to -105 mV upon perfusion of cAMP 10 µM and TMYX 6 mg/ml. Empty dots represent manual corrections of the applied voltage, used to measure the shift. (**B**) Sample I_f current traces recorded in control, in the presence of cAMP 10 µM, and during TMYX 6 mg/ml perfusion.

Since the effect of TMYX is modified by alterations in intracellular cAMP concentration (**Figure 3**), but TMYX does not block the channel alone, an interaction between TMYX and cAMP was therefore supposed. To verify this hypothesis, the macro-patches were perfused with solutions containing different cAMP concentrations, and the I_f current reduction was quantified as a shift of the AC in the presence of TMYX 6 mg/ml.

An experiment similar to that of **Figure 5** was performed, but I now also tested the effect of cAMP (1 µM) in combination of TMYX. cAMP 1 µM was first delivered alone and an increased in the current was observed, then, still in the presence of cAMP, TMYX 6 mg/ml was added and the effect of cAMP was reduced. This behavior can be appreciated both in the time course (**Figure 6A**) and in the sample current traces (**Figure 6B**).

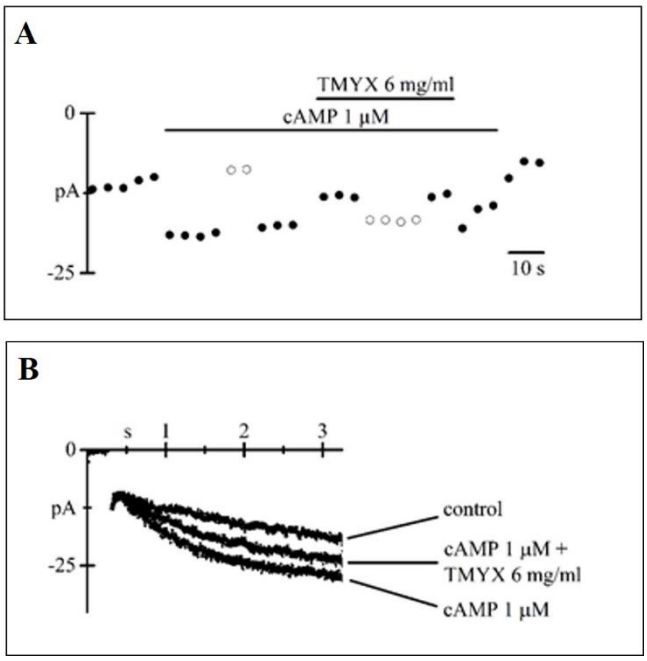

Figure 6. TMYX reduces the I_f current in inside-out configuration when delivered in the presence of cAMP 1 µM. (**A**) Sample time course of the I_f current amplitude during steps to -105 mV upon perfusion of cAMP 1 µM alone, to verify the integrity of the patch, and in combination with TMYX 6 mg/ml. Empty dots represent manual corrections of the applied voltage, used to measure the AC shift. (**B**) Sample I_f current traces recorded in control, in the presence of cAMP 1 µM alone and in combination with TMYX 6mg/ml.

The same experiment shown in **Figure 6** was repeated with a higher cAMP concentration (10 µM) and the reducing effect of TMYX was smaller. The time-course of the current amplitude (**Figure 7A**) and the I_f current traces (**Figure 7B**) show the reduction induced by TMYX 6 mg/ml.

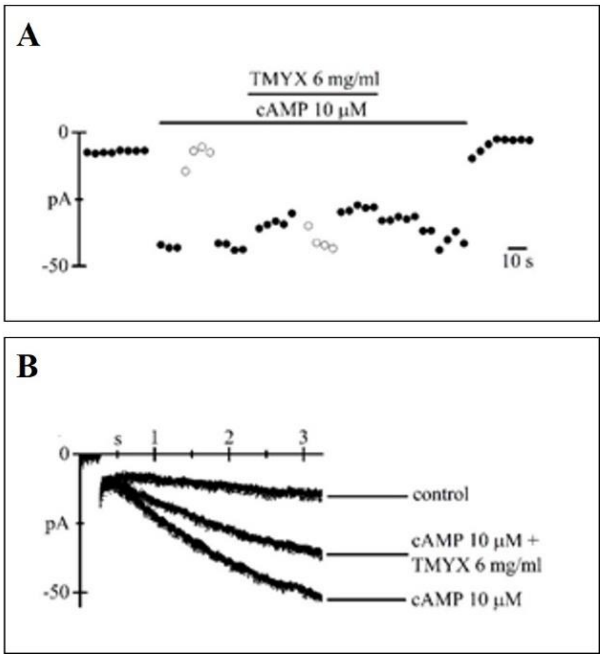

Figure 7. TMYX reduces the I_f current in inside-out configuration when delivered in the presence of cAMP 10 µM. (**A**) Sample time course of the I_f current amplitude during steps to -105 mV upon perfusion of cAMP 10 µM alone and in combination with TMYX 6 mg/ml. Empty dots represent manual corrections of the applied voltage, used to measure the AC shift. (**B**) Sample I_f current traces recorded in control, in the presence of cAMP 10 µM alone and in combination with TMYX 6 mg/ml.

The cAMP concentration was then raised to saturating levels (100 µM, **Figure 8**). The time-course of the I_f current amplitude (**Figure 8A**) and sample trace recordings (**Figure 8B**) demonstrate that in this condition TMYX is not able to elicit any blocking effect since no difference between cAMP 100 µM and TMYX 6 mg/ml + cAMP 100 µM was observed. These results thus suggest that TMYX cannot elicit any effect when cAMP is strongly activating (saturating concentration) the pacemaker channels.

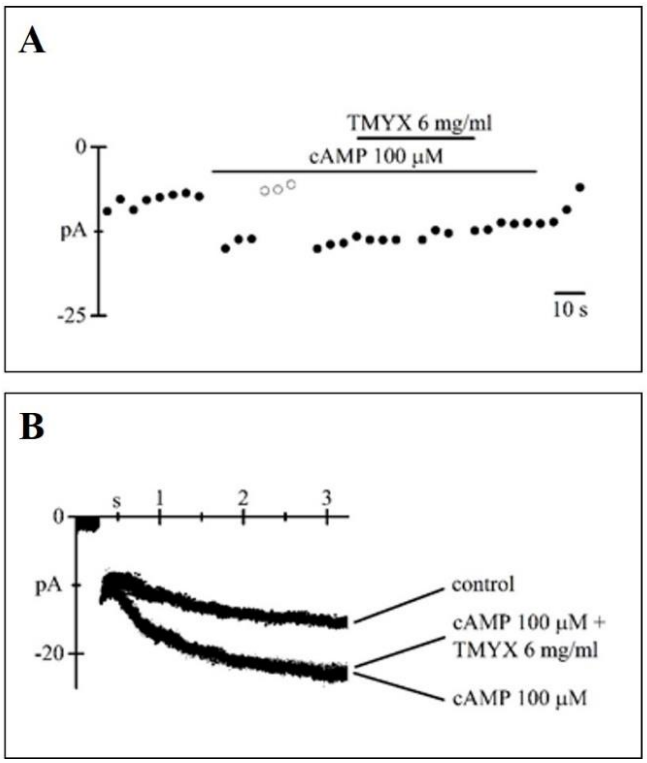

Figure 8. TMYX does not reduce the I_f current in inside-out configuration when delivered in the presence of saturated concentration of cAMP. (**A**) Sample time-course of the I_f current amplitude during steps to -105 mV upon perfusion of cAMP 100 µM alone and in combination with TMYX 6 mg/ml. Empty dots represent manual corrections of the applied voltage, used to measure the AC shift. (**B**) Sample I_f current traces recorded in control, in the presence of cAMP 100 µM alone, and in the presence of TMYX 6mg/ml.

In-vivo experiments:

ECG radio-telemetric recordings were performed in freely-moving mice to confirm and extend the information obtained with the *in-vitro* experiments. *In-vitro* single-cell experiments indeed represent a simplified study model able to provide insights into the effects of TMYX in a more physiological setting. The need to evaluate *in-vivo* effects in a variety of different conditions is particularly relevant for complex drugs, such as TMYX, which are composed by several individual compounds and can therefore act on multiple targets, in this case most likely not limited to the SAN area and to pacemaker cells.

We therefore set up *in-vivo* experiments in order to study the effects of TMYX on the intrinsic cardiac rate, accomplished by pharmacological denervation of the SAN. The aim of these experiments was to verify whether the bradycardic effect of TMYX observed in isolated SAN cells could also be reproduced in the intact animal when deprived of any autonomic modulation. A sample recording where TMYX was injected following muscarinic and β-adrenergic block (i.p. injection of atropine, 2 mg/kg and propranolol 1 mg/kg) is shown in **Figure 9**.

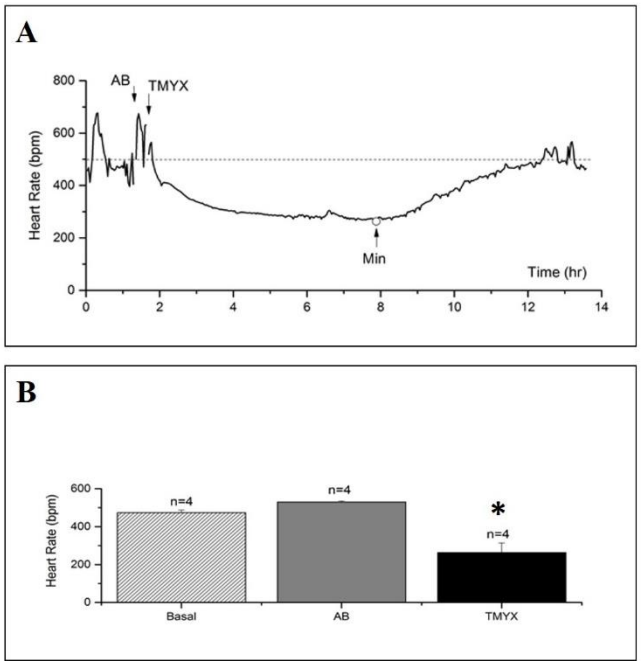

Figure 9. TMYX reduces the intrinsic heart rate in freely-moving mice. (**A**) Time-course of the heart rate recorded from a mouse in a typical experiment; each point represents the mean heart rate calculated over a period of 2 minutes. TMYX (5 g/kg) was injected i.p after about 30 minutes the induction of Autonomic Block (AB, arrow, i.p. Atropine 2 mg/kg + Propranolol 1 mg/kg). (**B**) Bar-graph showing mean heart rate values calculated for the three conditions and indicating steady-state rates in the mice before any treatment (Basal), after autonomic blockade (AB), and the minimal rate reached after drug injection (TMYX). n=4; *P<0.05, One-way ANOVA.

Following the attainment of a stable intrinsic rate (30 minutes after the AB induction), TMYX was administered and caused a marked, slow decay of the intrinsic heart rate. The slow rate persisted for several hours and was followed by a slow recovery. Mean rates (n = 4) shown in **Figure 9B** were: basal (measured prior to any pharmacological intervention): 474.1±12.0 bpm; intrinsic/AB (measured during AB): 529.6±5.7 bpm; and with TMYX (the minimal rate value after injection of TMYX and in the presence of a background AB): 263.6±50.5 bpm. The minimal rate in the presence of TMYX was 50.2% slower than basal rate and this effect occurred an average 445.2±84.7 minutes after drug administration. Statistical analysis showed that TMYX rate was significantly lower than both Basal and intrinsic/AB rates, and that Basal and intrinsic rates were similar.

Control experiments where a saline solution was used instead of TMYX (n=6) were carried out to confirm that the experimental manipulation (including the i.p. injection procedure) does not affect rate; in this case the heart rate was not significantly reduced (data not shown, P>0.05, t-test).

We next evaluated whether the slowing of the intrinsic heart rate induced by TMYX was maintained in the presence of intact autonomic control. To this aim a protocol similar to the one

described in **Figure 9** was used; since in this case no pharmacological block was required, a saline solution was injected as a control prior to the injection of TMYX. Unexpectedly, under these conditions TMYX induced a long lasting tachycardic effect (**Figure 10A**). The mean basal rate measured in 4 mice was 439.1±17.4 bpm before TMYX and it accelerated to 716.7±14.1 bpm in the presence of TMYX (**Figure 10B**).

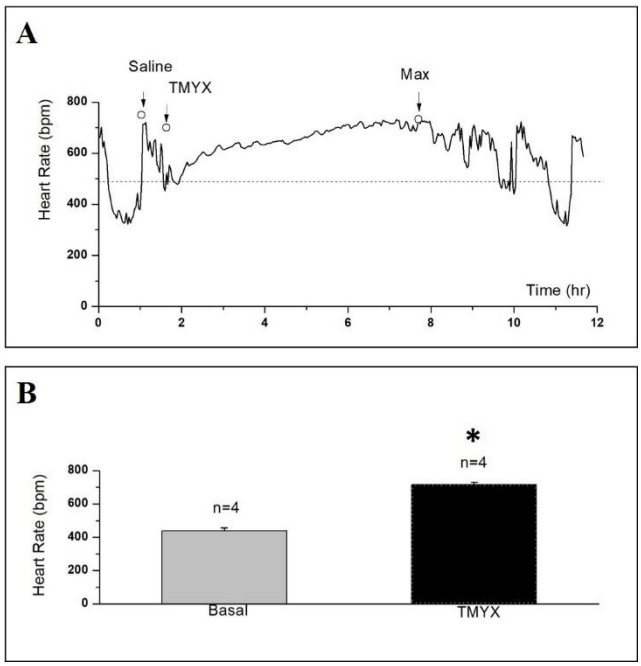

Figure 10. TMYX accelerates heart rate in freely-moving mice. (**A**) Time-course of heart rate recorded in a typical experiment; each point is the mean heart rate calculated over a period of 2 minutes. TMYX (5 g/kg) was injected after about 30 minutes from the injection of a saline solution. (**B**) Bar-graph showing mean heart rate values (bpm) calculated for the 2 conditions and indicating steady-state rates before any treatment (Basal) and the maximal rate reached after drug administration (TMYX). n=4; Student's t-test, *P<0.05.

This tachycardic action could be due either to a vagal inhibition or to a sympathetic potentiation or both. To identify the exact mechanism we carried out experiments in which the effect of TMYX was tested during either muscarinic or β-adrenergic block.

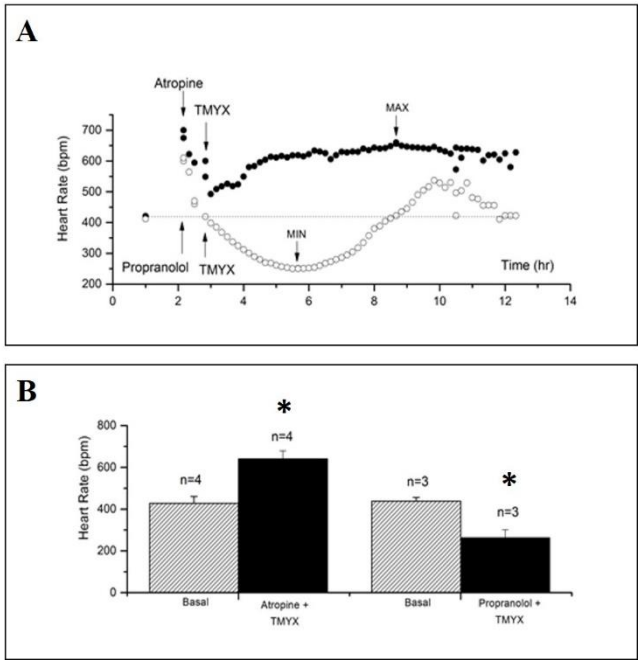

Figure 11. TMYX accelerates heart rate in the presence of the only sympathetic system while it decreases heart rate in the presence of parasympathetic system. (**A**) Time courses of heart rate recorded in two mice in the presence of TMYX following the pre-treatment with atropine (parasympathetic block) or propranolol (sympathetic block). For a direct comparison the two time courses are plotted on the same x-axis. The dashed line represents the basal heart rate measured as the mean heart rate during the first two hours of each experiment and are indicated by two points plotted conventionally at t=1 hr; all other points represent mean rate values calculated over a period of 10 minutes. (**B**) Bar-graph indicating basal, maximum (Atropine + TMYX) and minimum (Propranolol + TMYX)) heart rate values. *P<0.05; Two-way ANOVA.

In **figure 11A** the time courses of heart rates recorded in two different mice are shown; in one mouse the effect of TMYX was evaluated after inducing sympathetic block (propranolol, empty circles), while in the other mouse the effect of the drug was evaluated after blocking the parasympathetic activity (atropine, filled circles); in both mice, TMYX was injected (i.p.) 30 minutes after the injection of the autonomic blocker. These experiments were repeated in 3-4 animals and mean data (**Figure 11B**) confirmed the presence of a dual effect of TMYX. Indeed, during sympathetic block, TMYX elicited a prolonged bradycardic action, while during parasympathetic block the opposite effect prevailed and rate accelerated.

We then tested the hypothesis that the tachycardic effect of TMYX on rate is due to facilitation of the release of catecholamines from the sympathetic nerve terminals and used guanethidine, a molecule known to interfere with catecholamine release, to test whether it could functionally antagonize the effect of TMYX, without compromising the receptor. In these experiments guanethidine was i.p. injected 30 minutes before TMYX. The sample recording shown in **Figure 12A** clearly illustrates that in the presence of guanethidine, the tachycardic action of TMYX was

antagonized, although not completely removed. To quantify the TMYX effect (or lack of) in this condition we calculated for each mouse the rate at the corresponding time point that identified the maximal heart rate during perfusion of TMYX pretreated with saline (**Figure 10**). In the presence of guanethidine, the mean rate was not significantly different than basal rate (+11.1 %, **Figure 12B**).

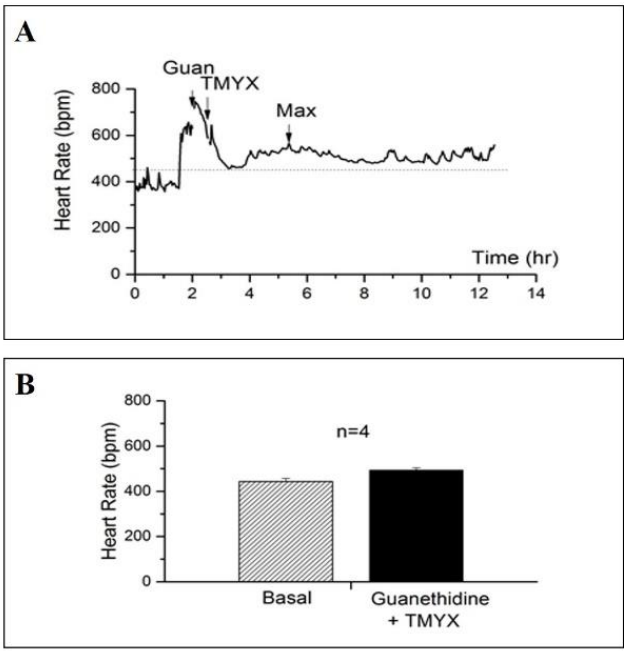

Figure 12. Guanethidine antagonizes the tachycardic action of TMYX. (**A**) Sample time course of heart rate recording in the presence of TMYX after pre-treatment with Guanethidine. (**B**) Bar-graph indicating mean basal and maximal HR measured in the presence of Guanethidine followed by TMYX. n=4; Student's t-test.

DISCUSSION

Traditional Chinese Medicine (TCM) is one of the oldest organized healing systems in the human history with an experience of 2-3000 years. The TCM approach is different from that of Western Medicine since it is based on a holistic view of both the diseased state and the associated therapy; western medicine, on the contrary, focusses on the identification of specific causes and therefore the therapeutic approach aims at removing the primary cause or, when this is not possible, at least at relieving the primary symptoms. Despite these differences, both approaches have reached high standard of applications due to a long history of proven results.

In this thesis project I decided to verify whether an approved TCM drug known to cure cardiac arrhythmic states exerts its effects on the primary determinants of cardiac rate, which are the cardiac pacemaker cells of the sinoatrial node (SAN).

The collaboration with the Chinese University of Tianjin has identified the drug TMYX as an interesting initial candidate since preliminary studies show that it may have a mechanism of action similar to that of Ivabradine (Servier, France), which is the unique pure bradycardic agent commercially available in western countries. I have previously described the first set of results obtained in our laboratory which are: 1) TMYX induces a dose-dependent reduction of action potentials, primarily due to a decrease of the slope of the diastolic depolarization (**Figure 1**) and 2) TMYX reduces the *funny* current (**Figure 2**).

These initial results raised the possibility of identifying new bradycardic agents. For this reason I carried out this research project in order to better understand the mechanism of action of this drug.

Since previous experiments had shown that the behavior of TMYX highly resembles that of a vagal release of ACh, I performed a series of experiments to evaluate if TMYX shares the pathway of ACh. Indeed ACh is the natural molecule that our organism uses to slow heart rate. ACh is a neuromodulator released by the parasympathetic system and its mode of action is quite complex and requires the initial stimulation of the membrane receptor muscarinic type 2 (M2 receptor) which then activates a series of enzymatic reactions that ultimately cause a decrease of the cAMP concentrations in the cell. cAMP is a key second messenger which, amongst its many action, it also directly interacts with the pacemaker channel: when cAMP is bound to pacemaker channels these channels are more likely to be open and pass more current, when cAMP is not bound to the channels the opposite occurs.

It was therefore clear that if TMYX acted like ACh, it somehow had to ultimately decrease the probability of cAMP interaction with pacemaker channels.

The first experiments confirmed that TMYX and ACh share a common mechanism, since the effect of the two substances on the *funny* current are not additive (**Figure 1**) and a following experiment

excluded that TMYX can bind to the M2 receptor because atropine (a blocker of the M2 receptor) does not alter the action of TMYX (**Figure 2**). The mechanism must therefore act somewhere downstream the receptor. In the course of the experiments in the whole-cell condition I noticed that when cAMP was maintained at a high concentration in the cytoplasm (**Figures 3**) the effect of TMYX was reduced. I therefore reasoned that it was possible that TMYX and cAMP were molecular antagonists. To really confirm this hypothesis I had to use the inside-out experiments since this was the only way in which the cAMP concentration could be controlled. I therefore run these experiments which confirmed that:

1) TMYX does not have any action on the channel when cAMP is absent (**Figures 4-5**);

2) TMYX decreases the pacemaker current when cAMP is present at non-saturating levels (**Figures 6-7**);

3) TMYX cannot decrease the pacemaker current when cAMP is at saturating high levels (**Figure 8**).

These 3 pieces of evidence definitively confirm that TMYX acts by antagonizing the effect of cAMP on the pacemaker channels.

TMYX is used by TCM doctors to treat cardiac conditions such as Left Ventricular Premature Beats (LVPB), Heart Failure (HF), and Coronary Artery Disease (CAD). The mechanism that I have identified is perfectly compatible with each of these disease; indeed CAD and HF are known to benefit from agents that slow heart rate. The reason for this beneficial effect of rate lowering agents is because reducing the rate of heart contraction reduces the metabolic consumption of the heart and also leaves more time for coronary flow during the prolonged diastolic time. Taken together these two aspects allow patients suffering from CAD and HF to benefit from rate lowering drugs.

These conclusions have been reached for other drugs thanks to important clinical trials enrolling thousands of patients. The mechanism identified by the *in-vitro* experiments is therefore nicely coherent with the reported clinical use of TMYX.

The case of LVPB is also extremely important. Indeed, this pathology arises mostly in the Purkinje fibres of the heart which are known to have the pacemaker phase and, if isolated from the SAN and AVN, can beat spontaneously. According to the literature LVPB arises when, for some reasons (possibly a higher than normal sympathetic stimulation and therefore increased cAMP levels), Purkinje cells becomes spontaneously active even in the presence of sinus rhythm. In this case therefore, in addition to the regularly triggered heart beats, the ventricle can occasionally present a premature additional beat. The mechanism leading to LVPB is perfectly compatible with the fact that TMYX can nicely treat this disease since it counteracts the action of the increased level of

cAMP observed in these patients and therefore impedes Purkinje cells to generate undesired and additional beats.

Furthermore, the antagonist action on the sympathetic activity is a key pharmacologic mechanism used by the β-blocker drugs. These drugs are widely used in the entire world to treat a large number of cardiac disease including CAD and HF. However, despite their widespread use, β-blocker drugs have some undesired and still unresolved side effects due to their mechanism of action[47,48]. Indeed β-blocker drugs act by binding to the β-adrenergic receptors and by doing this they block all the cascade resulting from receptor activation. In simple terms in the presence of β-blockers cAMP levels are decreased. This decrease is certainly beneficial for heart rate, because a smaller amount of cAMP will lead to less cAMP bound to the pacemaker channels and to a beneficial bradycardia. The often-undesired side effect of β-blockers is that a decrease amount of cAMP will also lead to a decreased cAMP-dependent phosphorylation of Calcium L-type channels as well as to many other different cAMP dependent effects. In the case of a decreased activation of Calcium L-type channels, the strength of contraction (inotropism) will be decreased, and in many cases this is undesired. For this reason, the search for molecules able to decrease heart rate, without modifying the strength of contraction is an incredible important aspect of the pharmacological research. According to my data it appears that the molecule of TMYX that acts on the pacemaker channel may have these characteristics and therefore it would be important to identify it. Indeed this molecule slows heart rate not by decreasing the cAMP levels, but by contrasting the action of cAMP on the pacemaker channels and therefore this would lead to a decrease of heart rate and a fully maintained strength of contraction.

The outcome of my research has identified the mechanism of action of one component of TMYX in *in-vitro* condition; however *in-vivo* experiments in mice suggested that there must be another bioactive molecule in TMYX with a different mode of action.

The *in-vivo* experiments performed in the presence of the autonomic block (**Figure 9**) showed a strong decrease of heart rate confirming the *in-vitro* results. However, when delivered in the intact animal TMYX can also raise heart rate (**Figure 10**). The latter experiments show that the tachycardic action was somehow elicited by the presence of only the sympathetic system (**Figure 11**). Experiments with Guanethidine revealed that TMYX may increase heart rate by favouring the release of Noradrenaline from sympathetic terminals. Further experiments are necessary to evaluate the action of this second molecule.

Taken together the results of this thesis clearly revealed the existence of almost two bioactive molecules in this TCM drug, a bradycardic agent and a tachycardic one. As explained above, these

molecules could have a high impact in the clinical settings. For this reason it would be important to isolate all the active molecules and tested them as we did for the entire drug.

GENERAL CONCLUSIONS

The two studies presented in this thesis highlight the importance of understanding the physiological mechanisms at the basis of the pacemaker activity, a fascinating phenomenon largely studied but also still widely unexplored.

Metabolic needs change during the life; for this reason even though the homeostatic balance of the chronotropic activity may at first appear as locked into stability, it should instead be considered a dynamic process. In the specific case of my thesis, the study of the physiological aging of the heart unravels some aspects of this process. Whether this research will pave the way to clinical application is a challenge that will require further basic studies.

The second study shows that drugs from the Traditional Chinese Medicine may represent an important new source of compounds capable of modifying the function of the pacemaker channels, and thus may represent novel antiarrhythmic agents potentially relevant also in the western medicine. In particular TMYX has the potential to act as a beta-blocker agent with a selectivity of action for the chronotropic activity.

MATERIALS AND METHODS

Animals

All procedures performed were in accordance with the Italian DL. 26/2014 and the European directive 2010/63/UE, regarding the protection of animals used for experimental and other scientific purposes. Mice and rabbits were obtain by commercial breeders (Charles River Laboratories International, Inc. and Envigo Laboratories Ltd.).

In-vivo experiments

Radio-telemetry system

Radio-telemetry system setup (Data Science International) is composed by: implantable radio-transmitters (TA10ETA-F20), receiver plates (RPC-1), a Data Exchange Matrix and a standard PC station. This system is capable of detecting and recording ECG signals, Temperature and Activity of mice.

Radio-transmitter implantation

For the surgical procedure mice were anesthetized with a mixture of isoflurane (Isoflurane-VET, Merial) 2% and oxygen 98%. The transmitter was implanted into the intraperitoneal cavity and the two electrodes were fixed one on the xiphoid process, near the ventricles, and the other one under the sternocleidomastoid muscle, near to the right atrium. Before and after the surgery, mice were injected with painkillers (Rimadyl 5mg/ml, Pfizer) and antibiotics (Baytril 2.5mg7ml, Bayer).

Experimental protocols

After the complete recovery of the mice, the registration protocols start. For the registration of Basal Heart Rates the signal was acquired for 2 minutes every 30 minutes. For the registration of Heart Rate in the presence of the substances of interest the registration was continuous.

We injected:

- Saline solution 0,9% NaCl as control;
- Atenolol (1mg/kg) or Propranolol (1mg/kg) as sympathetic blockers;
- Scopolamine (0.1mg/kg) or Atropine (2mg/kg) as parasympathetic blockers;
- Atenolol + Scopolamine or Propranolol + Atropine to totally block the autonomic system;
- Guanethidine (20mg/kg) to avoid noradrenergic release;
- Isoproterenol (0.2mg/kg) as sympathetic agonist;
- Carbachol (0.5mg/kg) as parasympathetic agonist.

Data analysis:

Dataquest 4.2 (Data Sciences International) was employed as the data acquisition software; analysis was carried out using LabChart 8.0 (ADinstruments) and OriginPro 2016 (Origin Lab). From the ECG analysis a tachogram, defined as the time course of the distance between subsequent R peaks, was generated. Heart rhythm (expressed in beats per minute, bpm) can be extrapolated from the RR distance.

Finally, HRV analysis was performed on the ECG traces. In the time domain, the root mean square of successive R-R interval differences (RMSSD, ms) was quantified; this index reflects short-term, high-frequency (HF) variations of RR interval, which are mainly due to cardiac parasympathetic activity. In the frequency-domain, the power spectrum was obtained with a fast Fourier transform-based method. The following parameters were quantified: the total power of the spectrum (ms^2), which reflects the overall variability; the power (ms^2) of the HF band; the low frequency (LF) to high frequency ratio (LF/HF), which estimates the fractional distribution of power and is taken as a synthetic measure of sympatho-vagal balance.

Different statistics were applicated for different experiments: two-way ANOVA test, one-way ANOVA test or Student's t-test. All values are given as mean ± the Standard Error of the Mean (SEM).

In-vitro **experiments**

Single sinoatrial node cells isolation

Mice were sacrificed by cervical dislocation. Rabbit were anesthetized by intramuscular injection of acepromazine (1 mg/Kg) and euthanized with intravenous injection of sodium thiopental (60 mg/Kg), and exsanguination. Hearts were extracted and bathed in pre-warmed (37°C) Tyrode solution (mM: NaCl, 140; KCl, 5.4; $CaCl_2$, 1.8; $MgCl_2$, 1; D-glucose, 5.5; Hepes-NaOH, 5; pH 7.4) containing 1000 U of heparin (Sigma-Aldrich). The SAN area was then exposed and dissected.

Tissue sections were subsequently washed 3 times in a solution containing NaCl 140 mM, KCl 5.4 mM, $MgCl_2$ 0.5 mM, KH_2PO_4 1.4 mM, taurine 50 mM, Hepes-NaOH 5 mM, D-glucose 5.5 mM (pH 6.9). Then the stripes were transferred in an enzymatic solution (NaCl 140 mM, KCl 5,4 mM, $MgCl_2$ 0.5 mM, KH_2PO_4 1.2 mM, Hepes NaOH 5 mM, taurine 50 mM, D-Glucose 5.5 mM, albumine 1 mg/ml, $CaCl_2$ 200 mM, collagenase (224 U/ml, for rabbit and 270 U/ml for mice; Worthington), elastase (1.42 U/ml, Sigma), and protease (0.45 U/ml, Sigma) at a temperature of 35°C for a variable period of time, usually ranging from 25 to 32 minutes. After this treatment, the tissue has been washed 3 times in a solution containing: KCl 20 mM; KOH 80 mM; albumine

1mg/ml, glutamic acid 70 mM; hydroxibutyric acid 10 mM; KH_2PO_4 10 mM; taurine 10 mM; Hepes-KOH 10 mM; EGTA-KOH 0.1 mM; pH 7.4. Cells were then dissociated with mechanical shacking for 5/10 minutes at 37°C in the same solution. Ca^{2+} was gradually reintroduced by adding increasing volumes of solution 6 (NaCl 10 mM, $CaCl_2$ 1.8 mM) and solution 5 (Tyrode solution containing albumin 1 mg/ml).

Finally, sinoatrial myocytes were left at 4°C the whole day.

Electrophysiological setup

A standard electrophysiological setup includes: an inverted microscope (Axiovert S100) placed on a vibration-damping table; an analog/digital interface (Digidata 1440, Axon Instruments); a microelectrode amplifier (Axopatch 200B, Axon Instruments); an amplifier headstage (CV-203BU, Axon Instruments); a mechanical micromanipulator; a temperature control system; a standard PC workstation with pClamp 10.7 software (Axon Instruments).

In order to isolate this setup from external electrical noises, all these devices are boxed in a Faraday cage.

Patch-clamp solutions

The extracellular solution used to record the I_f current was Tyrode solution plus $BaCl_2$ (1 µM) and $MnCl_2$ (2 µM) to improve I_f dissection over other ionic components. Tongmai Yangxin (TMYX), kindly provided by Zhongin Pharma (Tianjin Le Ren Tang Pharmaceutical Factory), was dissolved in water, warmed at 80°C for 15 minutes, filtered and used to prepare Tyrode solution. Electrophysiological experiments were performed using glass pipette with the resistance of about 5-8 mΩ filled with a solution containing (mmol/L): K-Aspartate, 130; NaCl, 10; EGTA-KOH, 5; $CaCl_2$, 2; $MgCl_2$, 2; ATP (Na-salt), 2; creatine phosphate, 5; GTP (Na-salt), 0.1; pH 7.2.

The inside-out configuration was obtained after Giga-seal formation, by removing the patch from the entire cell. The membrane was perfused with a control solution (mM: K-Asp, 130; NaCl, 10; CaCl2, 2; EGTA KOH, 5; Hepes KOH, 10; pH 7.2), and the pipette, with a resistance of 1-2 MΩ, was filled with the following solution (mM: NaCl, 70; KCl, 70; $CaCl_2$, 1.8; $MgCl_2$, 1; $BaCl_2$, 1; Hepes NaOH, 5; $MnCl_2$, 2; pH 7.4).

Data analysis and protocols

All data were acquired using pClamp 10.7 software and analyzed using Clampfit, OriginPro 2016 and GraphPad Prism 7 software.

The protocols used for *in-vitro* evaluations were designed on pClamp 10.7 software.

Action Potential

Action potentials were recorded in current-clamp configuration from single SA node cells or small uniformly-beating aggregates as continuous traces for several hundred seconds at a sampling rate of 2 KHz and filtered at 1 KHz with pClamp software. Raw AP records were digitally smoothed by a 10-point adjacent averaging smoothing procedure and the time derivative calculated according to a second polynomial, 8-point smoothing differentiating routine (Origin 7, Origin Lab, Northampton, MA).

Funny current

The classic protocol consists of a 1.2 sec hyperpolarization step from -35 to -75 mV in order to activate the current, followed by a 450 ms depolarizing step at +10 mV in order to ensure a complete closure of all channels.

The double step protocol consisted of 1.5 s voltage pulses to -125 mV, preceded by 0.75 s pulses to -65 mV, from a holding potential of -35 mV.

During these measurements, cells are perfused by a modified Tyrode solution to inactivate concurrent K^+ and Ca^{2+}-currents.

Funny current activation curve

The activation curve reflects the voltage-dependence of the channel. The holding potential for this protocol is set at -35 mV. It consists of a series of 10 mV hyperpolarizing steps from -35 to -125 mV, followed by a 1.5 sec step at -125 mV, where the chance of having HCN channels in open-state is 100%. Lastly, a step at +10 mV allows a complete closure of all channels. The length of the first hyperpolarizing step is gradually reduced from 12 to 4 seconds since the stabilization of the current gradually increases with hyperpolarization. Moreover, the cell suffers from remaining at those voltages for a long time.

Activation curves were fitted with the Boltzmann equation: $y=1/(1+\exp((V-V1/2)/s))$ where V is voltage, y the fractional activation, $V_{1/2}$ the half-activation voltage, and s the inverse-slope factor.

The statistic test used was Student's T test; $P < 0.05$.

Current density

Current density is defined as the amount of electric current per unit of cross section and it's measured in pA/pF. The statistic test used was Student's t-test; $P < 0.05$.

All data are presented as mean values ± SEM.

Inside-out configuration

After testing the integrity of the inside-out configuration by exposure to cAMP (10 μM) we evaluated the action of TMYX on the channel open probability, using a 60-s ramp protocol, from -35 to -145 mV. The ramp was sufficiently slow to allow the measurement of steady-state current, throughout the voltage range investigated. Macro-patch of I_f steady-state I-V relations were plotted after leakage correction. Probability curves and the curves were fitted with the Boltzmann equation.

BIBLIOGRAPHY

1. Harrison, D., Griendling, K.K., Landmesser, U., Hornig, B. & Drexler, H. Role of oxidative stress in atherosclerosis. *Am J Cardiol* **91**, 7A-11A (2003).
2. Gerszten, R.E. *et al.* MCP-1 and IL-8 trigger firm adhesion of monocytes to vascular endothelium under flow conditions. *Nature* **398**, 718-23 (1999).
3. Feske, S., Wulff, H. & Skolnik, E.Y. Ion channels in innate and adaptive immunity. *Annu Rev Immunol* **33**, 291-353 (2015).
4. Clemens, R.A. & Lowell, C.A. Store-operated calcium signaling in neutrophils. *J Leukoc Biol* **98**, 497-502 (2015).
5. Calejo, A.I. *et al.* Differences in the expression pattern of HCN isoforms among mammalian tissues: sources and implications. *Mol Biol Rep* **41**, 297-307 (2014).
6. Lakatta, E.G. & Sollott, S.J. Perspectives on mammalian cardiovascular aging: humans to molecules. *Comp Biochem Physiol A Mol Integr Physiol* **132**, 699-721 (2002).
7. Monfredi, O. & Boyett, M.R. Sick sinus syndrome and atrial fibrillation in older persons - A view from the sinoatrial nodal myocyte. *J Mol Cell Cardiol* **83**, 88-100 (2015).
8. Jose, A.D. & Collison, D. The normal range and determinants of the intrinsic heart rate in man. *Cardiovasc Res* **4**, 160-7 (1970).
9. Christou, D.D. & Seals, D.R. Decreased maximal heart rate with aging is related to reduced {beta}-adrenergic responsiveness but is largely explained by a reduction in intrinsic heart rate. *J Appl Physiol (1985)* **105**, 24-9 (2008).
10. Fleg, J.L. *et al.* Effects of acute beta-adrenergic receptor blockade on age-associated changes in cardiovascular performance during dynamic exercise. *Circulation* **90**, 2333-41 (1994).
11. Borer, J.S., Fox, K., Jaillon, P., Lerebours, G. & Ivabradine Investigators, G. Antianginal and antiischemic effects of ivabradine, an I(f) inhibitor, in stable angina: a randomized, double-blind, multicentered, placebo-controlled trial. *Circulation* **107**, 817-23 (2003).
12. Tardif, J.C. *et al.* Efficacy of ivabradine, a new selective I(f) inhibitor, compared with atenolol in patients with chronic stable angina. *Eur Heart J* **26**, 2529-36 (2005).
13. Fan, Y. *et al.* Analysis of bioactive components and pharmacokinetic study of herb-herb interactions in the traditional Chinese patent medicine Tongmai Yangxin Pill. *J Pharm Biomed Anal* **120**, 364-73 (2016).
14. Bennett, P.B., Yazawa, K., Makita, N. & George, A.L., Jr. Molecular mechanism for an inherited cardiac arrhythmia. *Nature* **376**, 683-5 (1995).
15. Rivolta, I. *et al.* Inherited Brugada and long QT-3 syndrome mutations of a single residue of the cardiac sodium channel confer distinct channel and clinical phenotypes. *J Biol Chem* **276**, 30623-30 (2001).
16. De Filippo, P., Ferrari, P., Iascone, M., Racheli, M. & Senni, M. Cavotricuspid isthmus ablation and subcutaneous monitoring device implantation in a 2-year-old baby with 2 SCN5A mutations, sinus node dysfunction, atrial flutter recurrences, and drug induced long-QT syndrome: a tricky case of pediatric overlap syndrome? *J Cardiovasc Electrophysiol* **26**, 346-9 (2015).
17. Mangoni, M.E. & Nargeot, J. Genesis and regulation of the heart automaticity. *Physiol Rev* **88**, 919-82 (2008).
18. Mangoni, M.E. *et al.* Functional role of L-type Cav1.3 Ca2+ channels in cardiac pacemaker activity. *Proc Natl Acad Sci U S A* **100**, 5543-8 (2003).
19. DiFrancesco, D., Ferroni, A., Mazzanti, M. & Tromba, C. Properties of the hyperpolarizing-activated current (if) in cells isolated from the rabbit sino-atrial node. *J Physiol* **377**, 61-88 (1986).

20. DiFrancesco, D. Pacemaker mechanisms in cardiac tissue. *Annu Rev Physiol* **55**, 455-72 (1993).
21. DiFrancesco, D. A study of the ionic nature of the pace-maker current in calf Purkinje fibres. *J Physiol* **314**, 377-93 (1981).
22. DiFrancesco, D. & Tortora, P. Direct activation of cardiac pacemaker channels by intracellular cyclic AMP. *Nature* **351**, 145-7 (1991).
23. Zagotta, W.N. *et al.* Structural basis for modulation and agonist specificity of HCN pacemaker channels. *Nature* **425**, 200-5 (2003).
24. Ulens, C. & Siegelbaum, S.A. Regulation of hyperpolarization-activated HCN channels by cAMP through a gating switch in binding domain symmetry. *Neuron* **40**, 959-70 (2003).
25. Chen, Y.J., Chen, S.A., Chang, M.S. & Lin, C.I. Arrhythmogenic activity of cardiac muscle in pulmonary veins of the dog: implication for the genesis of atrial fibrillation. *Cardiovasc Res* **48**, 265-73 (2000).
26. Vaca, L. *et al.* Mutations in the S4 domain of a pacemaker channel alter its voltage dependence. *FEBS Lett* **479**, 35-40 (2000).
27. Viscomi, C. *et al.* C terminus-mediated control of voltage and cAMP gating of hyperpolarization-activated cyclic nucleotide-gated channels. *J Biol Chem* **276**, 29930-4 (2001).
28. Accili, E.A., Proenza, C., Baruscotti, M. & DiFrancesco, D. From funny current to HCN channels: 20 years of excitation. *News Physiol Sci* **17**, 32-7 (2002).
29. Altomare, C. *et al.* Heteromeric HCN1-HCN4 channels: a comparison with native pacemaker channels from the rabbit sinoatrial node. *J Physiol* **549**, 347-59 (2003).
30. Ludwig, A., Zong, X., Hofmann, F. & Biel, M. Structure and function of cardiac pacemaker channels. *Cell Physiol Biochem* **9**, 179-86 (1999).
31. Seifert, R. *et al.* Molecular characterization of a slowly gating human hyperpolarization-activated channel predominantly expressed in thalamus, heart, and testis. *Proc Natl Acad Sci U S A* **96**, 9391-6 (1999).
32. Moroni, A. *et al.* Kinetic and ionic properties of the human HCN2 pacemaker channel. *Pflugers Arch* **439**, 618-26 (2000).
33. Wainger, B.J., DeGennaro, M., Santoro, B., Siegelbaum, S.A. & Tibbs, G.R. Molecular mechanism of cAMP modulation of HCN pacemaker channels. *Nature* **411**, 805-10 (2001).
34. Wang, J., Chen, S. & Siegelbaum, S.A. Regulation of hyperpolarization-activated HCN channel gating and cAMP modulation due to interactions of COOH terminus and core transmembrane regions. *J Gen Physiol* **118**, 237-50 (2001).
35. Brodde, O.E. & Michel, M.C. Adrenergic and muscarinic receptors in the human heart. *Pharmacol Rev* **51**, 651-90 (1999).
36. Walsh, D.A. & Van Patten, S.M. Multiple pathway signal transduction by the cAMP-dependent protein kinase. *FASEB J* **8**, 1227-36 (1994).
37. Kaumann, A.J. & Molenaar, P. Modulation of human cardiac function through 4 beta-adrenoceptor populations. *Naunyn Schmiedebergs Arch Pharmacol* **355**, 667-81 (1997).
38. Pumprla, J., Howorka, K., Groves, D., Chester, M. & Nolan, J. Functional assessment of heart rate variability: physiological basis and practical applications. *Int J Cardiol* **84**, 1-14 (2002).
39. Larson, E.D., St Clair, J.R., Sumner, W.A., Bannister, R.A. & Proenza, C. Depressed pacemaker activity of sinoatrial node myocytes contributes to the age-dependent decline in maximum heart rate. *Proc Natl Acad Sci U S A* **110**, 18011-6 (2013).
40. Ferrara, N. *et al.* beta-adrenergic receptor responsiveness in aging heart and clinical implications. *Front Physiol* **4**, 396 (2014).
41. Hotta, H. & Uchida, S. Aging of the autonomic nervous system and possible improvements in autonomic activity using somatic afferent stimulation. *Geriatr Gerontol Int* **10 Suppl 1**, S127-36 (2010).

42. Yaniv, Y. *et al.* Deterioration of autonomic neuronal receptor signaling and mechanisms intrinsic to heart pacemaker cells contribute to age-associated alterations in heart rate variability in vivo. *Aging Cell* **15**, 716-24 (2016).
43. Huang, X., Yang, P., Yang, Z., Zhang, H. & Ma, A. Age-associated expression of HCN channel isoforms in rat sinoatrial node. *Exp Biol Med (Maywood)* **241**, 331-9 (2016).
44. Esler, M. *et al.* Sympathetic nerve biology in essential hypertension. *Clin Exp Pharmacol Physiol* **28**, 986-9 (2001).
45. Milanesi, R., Baruscotti, M., Gnecchi-Ruscone, T. & DiFrancesco, D. Familial sinus bradycardia associated with a mutation in the cardiac pacemaker channel. *N Engl J Med* **354**, 151-7 (2006).
46. Kobinger, W. & Lillie, C. Specific bradycardic agents--a novel pharmacological class? *Eur Heart J* **8 Suppl L**, 7-15 (1987).
47. Yusuf, S. & Camm, A.J. Sinus tachyarrhythmias and the specific bradycardic agents: a marriage made in heaven? *J Cardiovasc Pharmacol Ther* **8**, 89-105 (2003).
48. DiFrancesco, D. & Camm, J.A. Heart rate lowering by specific and selective I(f) current inhibition with ivabradine: a new therapeutic perspective in cardiovascular disease. *Drugs* **64**, 1757-65 (2004).